

# Supporting information

## Contents

|  |    |
|--|----|
| List of abbreviations .....                  | 2  |
| Materials and instrumentation.....           | 3  |
| Experimental .....                           | 4  |
| Self-assembly and shape transformation.....  | 8  |
| Dynamic Light Scattering .....               | 11 |
| Circular Dichroism measurements.....         | 12 |
| Spectra of NMR spectroscopy, GPC and CD..... | 14 |
| TEM and Cryo-TEM images .....                | 19 |
| Behaviour of the membrane study .....        | 26 |
| Stability and degradation study .....        | 31 |
| References.....                              | 40 |

## List of abbreviations

|                  |   |
|------------------|---|
| BCP              | Block copolymer   |
| CD               | Circular Dichroism Spectroscopy                         |
| CO <sub>2</sub>  | Carbon dioxide  |
| (Cryo)TEM        | (Cryogenic) Tunnelling Electron Microscopy              |
| DLS              | Dynamic Light Scattering                                |
| DMF              | N,N-Dimethyl formamide                                  |
| DSC              | Differential Scanning calorimetry                       |
| GPC              | Gel Permeation Chromatography                           |
| HFIP             | Hexafluorisopropanol                                    |
| H <sub>2</sub> O | Hydrogen dioxide  |
| MilliQ           | Ultra-pure water  |
| NCA              | N-carboxyanhydride                                      |
| PBLG             | Poly( $\gamma$ -benzyl-L-glutamate)                     |
| PBLG-b-PSar      | Poly( $\gamma$ -benzyl-L-glutamate)-block-polysarcosine |
| PEG              | Polyethylene glycol                                     |
| PSar             | Polysarcosine   |
| ROP              | Ring opening polymerisation                             |
| RT               | Room temperature ( $\sim 20$ °C)                        |

## Materials and instrumentation

All chemicals used were of commercial grade and used directly without purification.

$^1\text{H}$  and DOSY spectra were measured on an ASCEND 400 BRUKER apparatus in  $\text{CDCl}_3$  and MeOD. J values are given in Hz.

TEM images were recorded on JEOL TEM 1400 on carbon copper grids.

CryoTEM images were recorded on JEOL 2100.

DLS measurements were done on the DLS zetasizer pro in MilliQ water.

Osmolality was measured on Gonotec Osmat 3000.

CD measurements were done on JASCO J-815 CD.

DSC measurements were performed on the DSC822<sup>e</sup> with the TSO 801RO Sample Robot from Mettler Toledo.

The polydispersity was determined with Shimadzu GPC with THF as a solvent.

Fluorescence spectroscopy was measured on JASCO FP-8300ST.

The centrifuges used to spin down product were the HERMLE Z306 for falcon tubes and Centrifuge 5430 R for Eppendorfs.

CMC was determined to on NanoSight LM10.

## Experimental

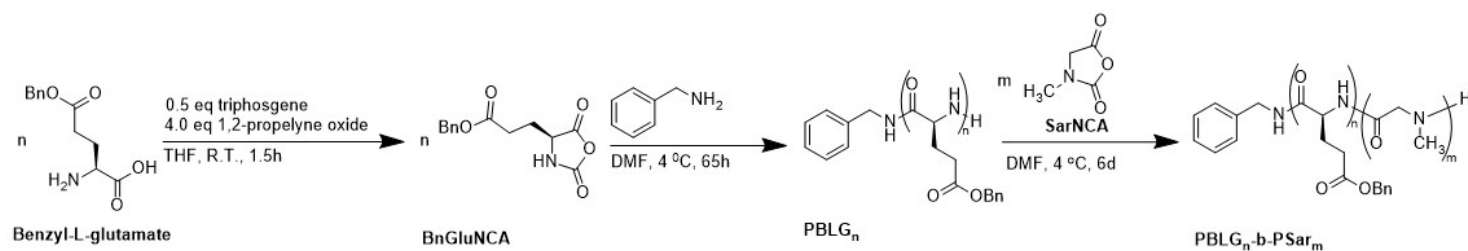


**Figure S1:** Overall scheme of  $PBLG_n$ - $b$ - $PSar_m$  preparation.

### Synthesis benzyl glutamate NCA

$\gamma$ -Benzyl-L-glutamate (1.51 g, 6.36 mmol, 1 eq), THF (30 mL) and 1,2-propylene oxide (4 eq) were added to a flask under continuous stirring. Subsequently, triphosgene (1.012 mg, 3.31 mmol, 0.54 eq) was added in one portion to the flask.  $\gamma$ -Benzyl-L-glutamate dissolved with noticeable heat release. The mixture was stirred at room temperature for 1.5 h and subsequently cooled to 0 °C. Thereafter, ice chilly water (30 mL) was added to the mixture to quench any excess phosgene. The mixture was stirred for 3 min, to release CO<sub>2</sub> gas. Argon was bubbled through the mixture for a period of 15 min to quench excess phosgene. The mixture was then extracted with ethyl acetate (2 x 30 mL). The combined organic layers were extracted with brine (2 x 30 mL) and dried over anhydrous Na<sub>2</sub>SO<sub>4</sub>. The product was concentrated under vacuo, which was further dried on high vacuum for 16h to obtain **BnGluNCA** as a white powder (1.60 g, 5.34 mmol, 95.2% yld). The product was stored at -20 °C.

<sup>1</sup>HNMR (400 MHz, CDCl<sub>3</sub>)  $\delta$  7.4-7.33 (m, 5H, Ar-H), 6.35 (s, 1H, NH), 5.14 (s, 2H, CH<sub>2</sub>), 4.39-4.35 (t, 1H, CH), 2.62-2.09 (m, 2H, CH<sub>2</sub>)

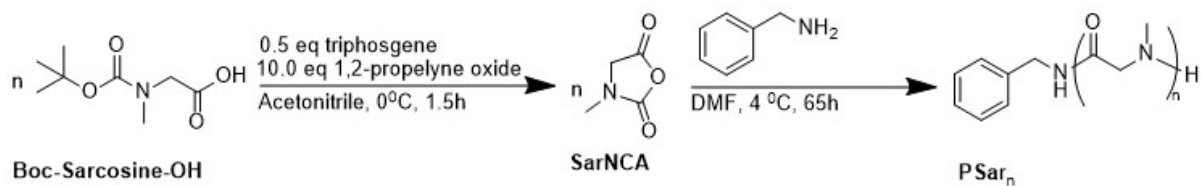


**Figure S2:** Overall scheme of SarNCA synthesis and subsequent polymerisation of PSar.

## Synthesis sarcosine NCA

Boc-Sar-OH (1.276 g, 6.74 mmol, 1 eq) and 1,2-propylene oxide (4.7 mL, 67.1 mmol, 10.0 eq) were dissolved in dry acetonitrile (30 mL). Finally, triphosgene (1.080 g, 3.64 mmol, 0.54 eq) was added in one portion to the mixture. Two needles were stuck into the septum in order to facilitate in situ deprotection of Boc-Sar-OH under a constant stream of argon. The mixture was stirred while cooled on ice for 1.5 h. After completion, ice chilly water (15 mL) was added to the reaction mixture to quench any excess phosgene in the mixture and stirred for an additional 5 minutes. The resulting mixture was extracted with ethyl acetate (2 x 30 mL). The combined organic phase was subsequently washed with brine (3 x 30 mL). The organic phase was dried over anhydrous Na<sub>2</sub>SO<sub>4</sub>. The product was concentrated in vacuo. A transparent oil was obtained and subsequently dried for 16h on high vacuum to obtain white crystals **SarNCA** (527.7 mg, 4.59 mmol, 68.0% yld) as a white powder. The product was stored at -20 °C.

<sup>1</sup>HNMR (400 MHz, CDCl<sub>3</sub>) δ 4.13 (s, 2H, CH<sub>2</sub>), 3.05 (s, 3H, CH<sub>3</sub>)

## Synthesis of PBLG<sub>40</sub>

**BnGluNCA** (202.7 mg, 0.77 mmol, 40 eq) was dissolved in dry DMF (3 mL) under a continuous Ar flow. Subsequently, a solution of 0.0366 mM benzylamine in dry DMF (0.52 mL, 0.019 mmol, 1 eq) was added to the solution. The reaction mixture was stirred for 70 h at 4 °C. Thereafter, the mixture was carefully pipetted into stirred, ice cold diethyl ether (150 mL). The white precipitates were separated through centrifugation and subsequently freeze dried from H<sub>2</sub>O/1,4-dioxane 50:50 to obtain **PBLG<sub>40</sub>** (146.3 mg, 0.016 mmol, 86.7 %yld) as a fluffy white powder.  $\bar{M}_n$  was 1.04 as determined by GPC with THF as eluent.

<sup>1</sup>HNMR (400 MHz, CDCl<sub>3</sub>)  $\delta$  8.30 (bs, NH), 7.32-7.19 (m, Ar-H), 5.37 (s, 79H, Ar-CH<sub>2</sub>NH), 4.34 (bs, 76H, CH<sub>2</sub>-Ar), 3.93 (bs, 33H, CH), 2.57-2.12 (m, 154 H, CH<sub>2</sub>)

## Synthesis of PBLG<sub>40</sub>-b-pSar<sub>50</sub>

**PBLG<sub>40</sub>** (149.9 mg, 0.0169 mmol, 1 eq) was dissolved in dry DMF (1 mL) and cooled to 0 °C. **SarNCA** (97.2 mg, 0.884 mmol, 50 eq) was dissolved in dry DMF under constant argon flow. Subsequently, the **PBLG<sub>40</sub>** solution in DMF was added to the monomer solution of **SarNCA** under argon flow. The mixture was stirred at 4 °C for 5 days. Thereafter, the mixture was carefully pipetted into stirred, ice cold diethyl ether (50 mL). The white precipitates were separated by centrifugation and subsequently washed with diethyl ether (2 x 50 mL). The precipitates were freeze dried from H<sub>2</sub>O/1,4-dioxane 50:50 to obtain **PBLG<sub>40</sub>-b-PSar<sub>50</sub>** (176.5 mg, 0.0142 mmol, 84.0 %yld) as a fluffy white powder.  $\bar{M}_n$  was 1.07 determined by GPC with dimethylacetamide as eluent.

<sup>1</sup>HNMR (400 MHz, CDCl<sub>3</sub>)  $\delta$  8.30 (bs, NH), 7.29-7.23 (m, ArH), 5.02 (s, 80H, Ar-CH<sub>2</sub>NH), 4.52 (bs, 2H, CH<sub>2</sub>-Ar), 3.02 (bs, 150H, CH<sub>3</sub>), 2.56-2.09 (m, CH<sub>2</sub>)

## Synthesis of pSar<sub>40</sub>

**SarNCA** (134.1 mg, 1.16 mmol, 44 eq) was dissolved in dry DMF (5 mL) under argon and subsequently cooled to 0 °C. Benzyl amine (3μL, 0.03 mmol, 1eq) was dissolved in dry DMF (3 mL) and cooled to 0 °C. Thereafter, the benzyl amine solution was added to the SarNCA solution under a constant stream of Ar. The resulting mixture was stirred for 90 h at 4 °C. After completion, the solution was slowly pipetted on ice cold diethyl ether (50 mL). The white precipitates were separated by centrifugation and washed with diethyl ether (3 x 50 mL). Then, the precipitates were freeze dried from H<sub>2</sub>O to obtain **PSar<sub>40</sub>** (214,7 mg, 0.073 mmol, 12.1%) as a slightly yellow solid.  $\bar{M}_n$  was determined to be 1.04 by GPC with THF as eluent.

**<sup>1</sup>H NMR** (400 MHz, MeOD)  $\delta$  7.38 – 7.26 (m, 5H), 4.47 – 4.02 (m, 75H), 2.98 (td,  $J = 23.4, 14.7$  Hz, 143H), 1.35 (d,  $J = 3.2$  Hz, 2H).

# Self-assembly and shape transformation

## Preparation of BCPs polymersomes

Typically, the BCPs were dissolved in 1 ml DMF (4 mg/mL). MQ water (2 mL) was then added using Chymex syringe pumps over a period of 4 h (flow rate 0.5 mL/h) with an 11-minute delay interval under constant stirring to obtain a concentration of 1.33 mg/ml and 66% water content. After the 4 h period, MQ water (9 mL) was added in one portion to quench the self-assembly for a total concentration of 0.33 mg/ml in 92% water content. Subsequently, the mixture was spun down at 10,000 rpm for 10 min and the supernatant was discarded. The pellets were resuspended in MQ water (1 mL). This process was repeated two more times to obtain the washed self-assemblies.

## Shape transformation of BCPs

BCPs were dissolved in 1 ml DMF (4 mg/mL). MQ water (2 mL) was then added using Chymex syringe pumps over a period of 4 h (flow rate 0.5 mL/h) with an 11-minute delay interval under constant stirring. After the 4 h period, the sample was split into parts (1.33 mg/ml) with a 66% water content. While stirring, 2000 $\mu$ g of PEG2000<sup>1</sup> was added to the self-assembly (1 mg) before quenching by adding MQ water in one portion to quench the self-assembly after 1 minute to obtain 92% water content. Subsequently, the mixture was spun down at 10,000 rpm for 10 min. and the supernatant was discarded. The pellets were resuspended in MQ water (1 mL), and this process was repeated two more times to obtain the washed self-assemblies.

---

<sup>1</sup> Or 5 $\mu$ L of 400mg/ml PEG2000

## **Heated shape transformation of BCPs**

The heated shape transformation was performed through a similar method as the previously mentioned shape transformation. After the self-assembly was performed using the Chymex syringe pumps, the into four split samples were heated by being held in a water bath for 1 minute at the right temperature. After this minute, 2000 $\mu$ g of PEG2000 was inserted into the sample and quenched after a range of times to obtain 92% water content. In the same fashion as described prior, the mixture was spun down at 10,000 rpm for 10 min. and the supernatant was discarded. The pellets were resuspended in MQ water (1 mL), and this process was repeated two more times to obtain the washed self-assemblies.

## **Induced shape transformation**

Saccharose and the homopolymer of sarcosine were used in a similar fashion to PEG2000 to induce a shape transformation. The saccharose was added to the split sample (1 mg) and quenched with water after 1 minute to obtain 92% water content. The work up to obtain the washed self-assemblies was done in the same fashion as described prior.

## **PSar homopolymer shape transformation**

The (heated) shape transformation of PSar and the polymersome formation was performed in the same manner as the earlier described method for BCP.

## **Heated dialysis**

After the self-assembly was performed using the Chymex syringe pumps, the solution was transferred to a dialysis bag. The bag was added to a water bath with a temperature of 70 °C to perform the dialysis. Subsequently, the bag was transferred

to a new water bath at 70 °C after 5 minutes, 10 minutes, 15 minutes and finally after 20 minutes. Then, the dialysis bag was transferred to a room temperature water bath and stirred for an additional hour. Finally, the mixture was spun down at 10,000 rpm for 10 min. and the supernatant was discarded. The pellets were resuspended in MQ water (1 mL), this process was repeated two more times to obtain the washed self-assemblies.

## Osmometer

Osmolality is a measurement of the total number of solutes in a liquid solution expressed in osmoles of solute particles per kilogram of solvent.[1] This was done to give an indication of the osmotic strength of each of these solutions. The osmolality of the PEG<sub>44</sub>, PSar<sub>40</sub>, and saccharose solutions was measured at a concentration of 400 mg/ml (**Table S1**). Of each solution 50 µl was transferred to a 0.5 ml Eppendorf tube which was inserted in the osmometer.

*Table S1: Osmolality values of various samples.*

| Sample name  | Osmolality (mOsm/kg) |
|--------------|----------------------|
| PEG400       | 2243                 |
| 40PSar400    | 1129                 |
| 20PSar400    | 1217                 |
| Sacharose400 | 1649                 |

# Dynamic Light Scattering

**Table S2:** Average sizes of self-assembled structures of PBLG<sub>40</sub>-b-PSar<sub>50</sub> with different preparation methods. Experiments were performed in triplo on DLS zetasizer pro with general purpose analysis mode.

| Sample name  | Average size (nm) |
|--|-------------------|
| Polymersome  | 350.8             |
| Stomatocyte, quenched after 5 s of PEG addition <sup>a</sup>   | 460.2             |
| Stomatocyte, quenched after 30 s of PEG addition <sup>a</sup>  | 480.9             |
| Stomatocyte, quenched after 1 min of PEG addition <sup>a</sup> | 474.4             |
| Stomatocyte, quenched after 2 min of PEG addition <sup>a</sup> | 519.6             |
| Dialysis <sup>a</sup>  | 469.2             |
| Polymersome, freeze dried                                      | 361.3             |

<sup>a</sup> The shape transformations were performed at 70 °C

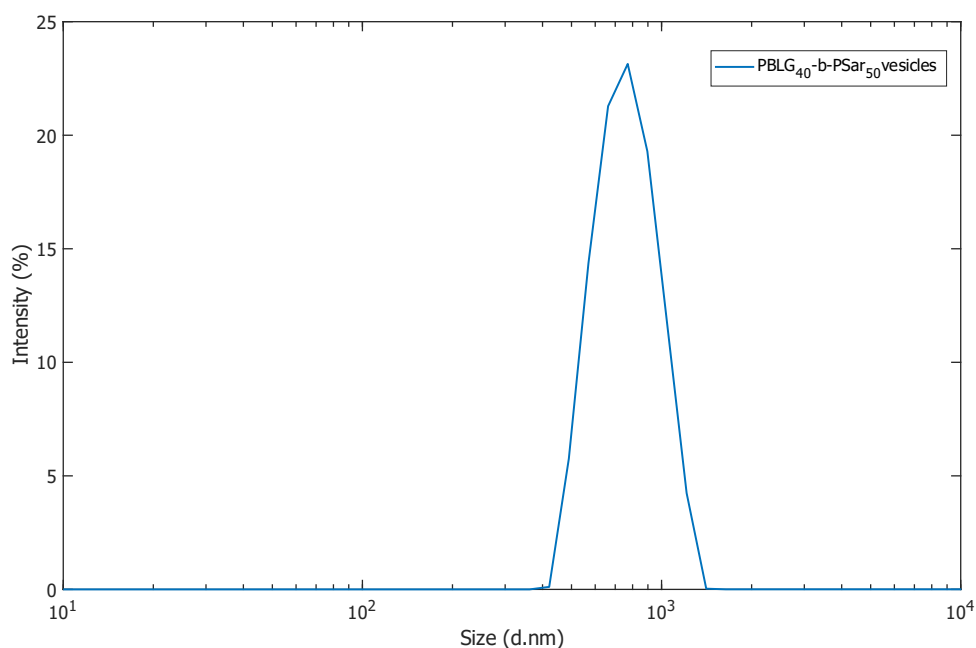


**Figure S3:** DLS polymersome vesicles peak.

## Circular Dichroism measurements

When the wavelength reaches 185 nm, the CD measurement is no longer accurate.

The parameters for these measurements include an accumulation of five measurements with a scanning speed of 200 nm/min and a D.I.T. of 0.5 seconds.

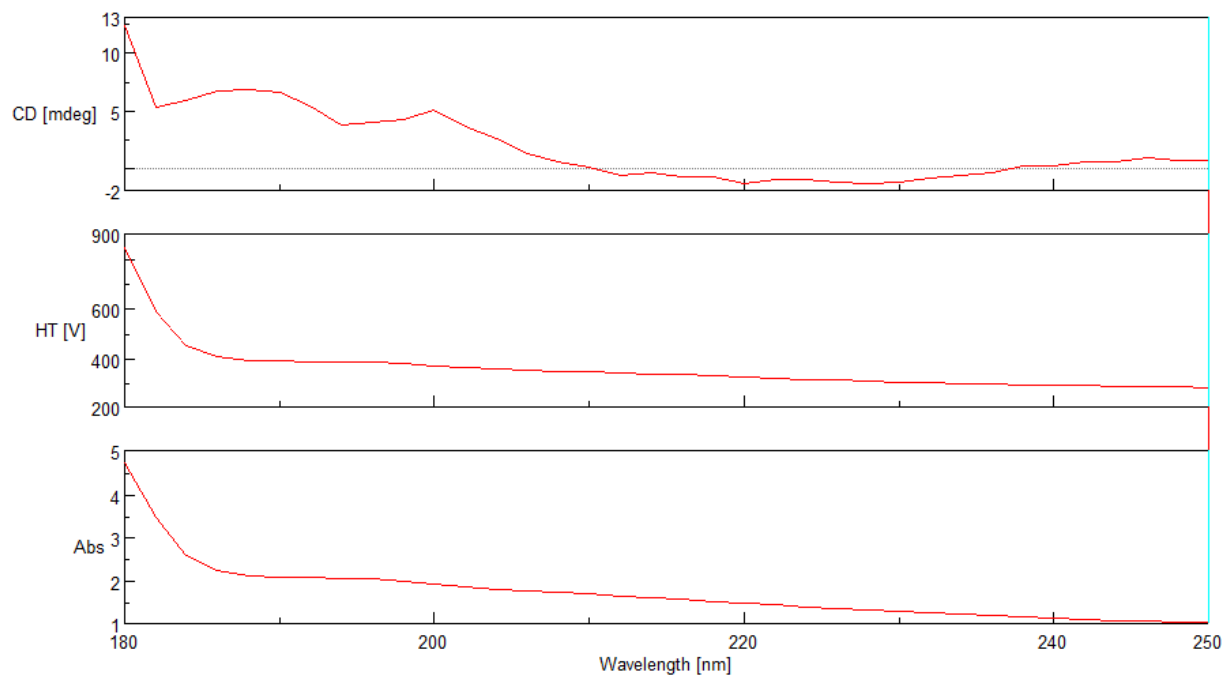


**Figure S4:** CD measurement of PBLG<sub>40</sub>-b-PSar<sub>50</sub> polymersomes.

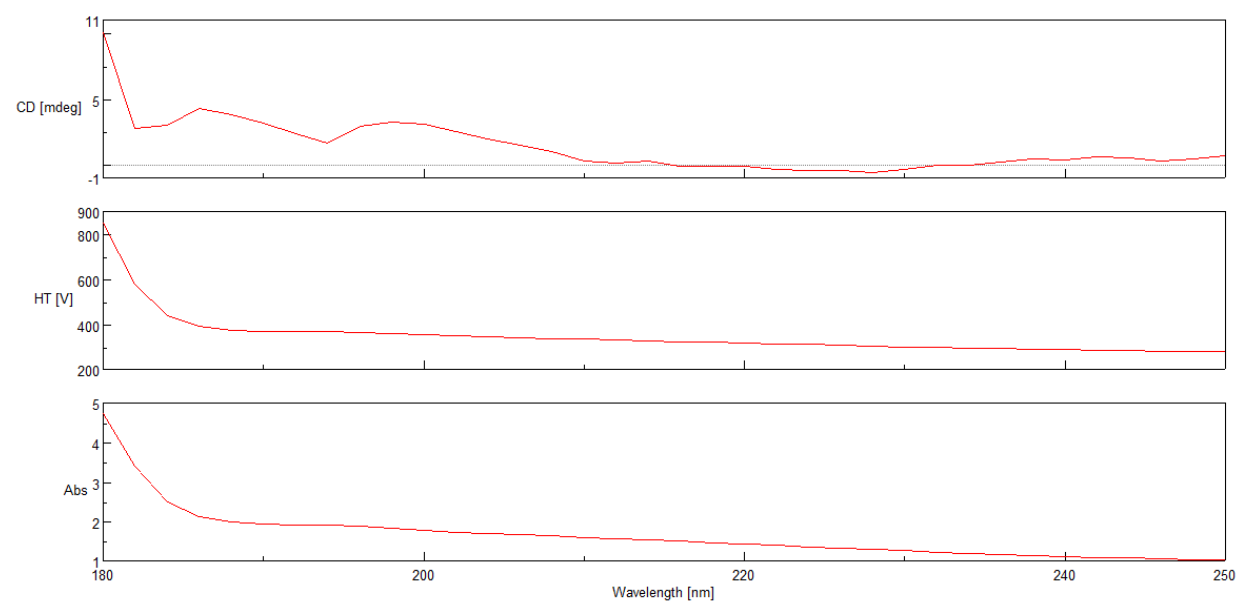


**Figure S5:** CD measurement of PBLG<sub>40</sub>-b-PSar<sub>50</sub> shape transformation at 70 °C, quenched after 30s.

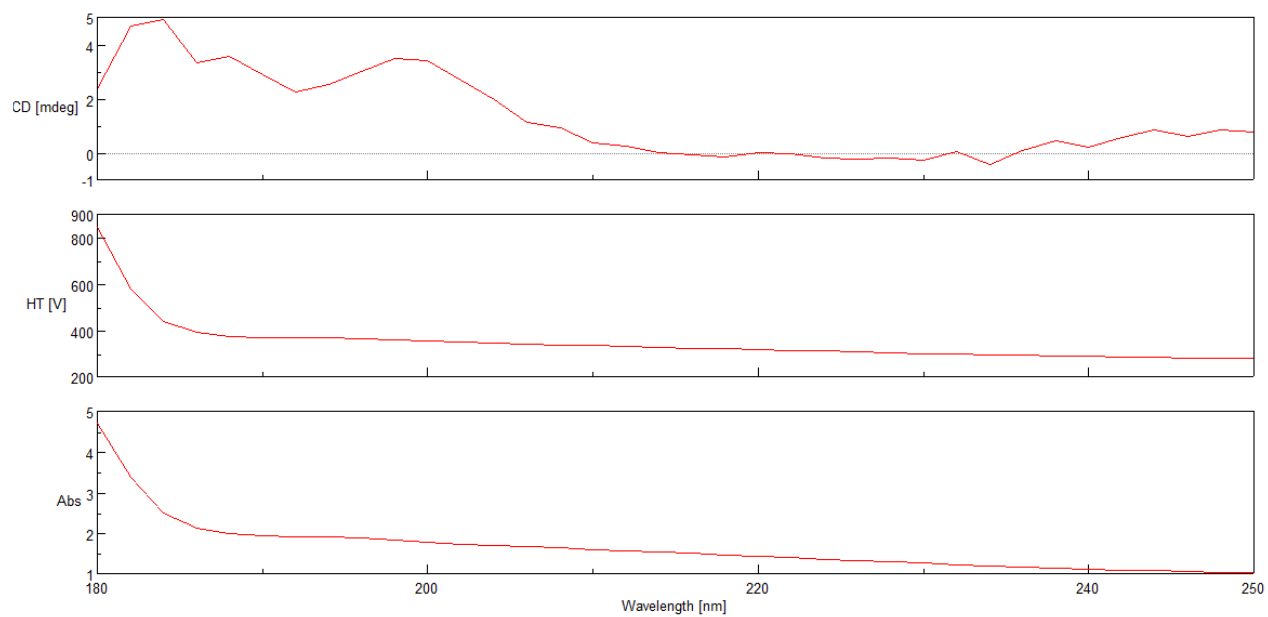


**Figure S6:** CD measurement of PBLG<sub>40</sub>-b-PSar<sub>50</sub> shape transformation at 70 °C, quenched after 1 min.

# Spectra of NMR spectroscopy, GPC and CD

## 400 MHz NMR

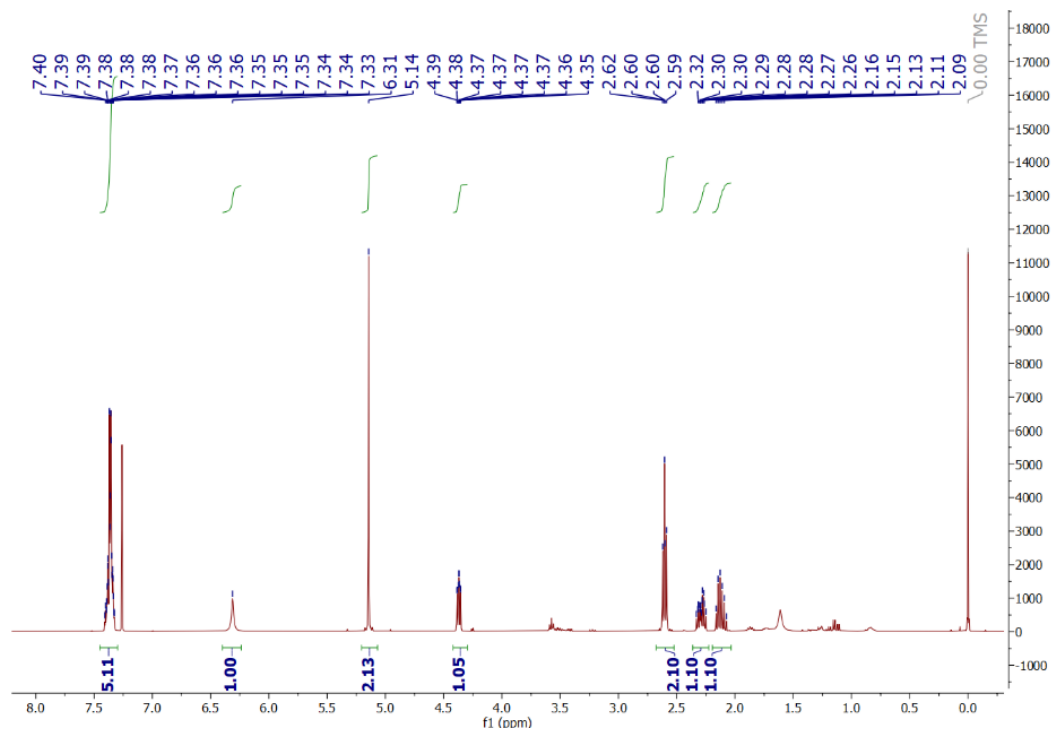


Figure S7:  $^1\text{H}$  NMR spectrum of BnGlu NCA.

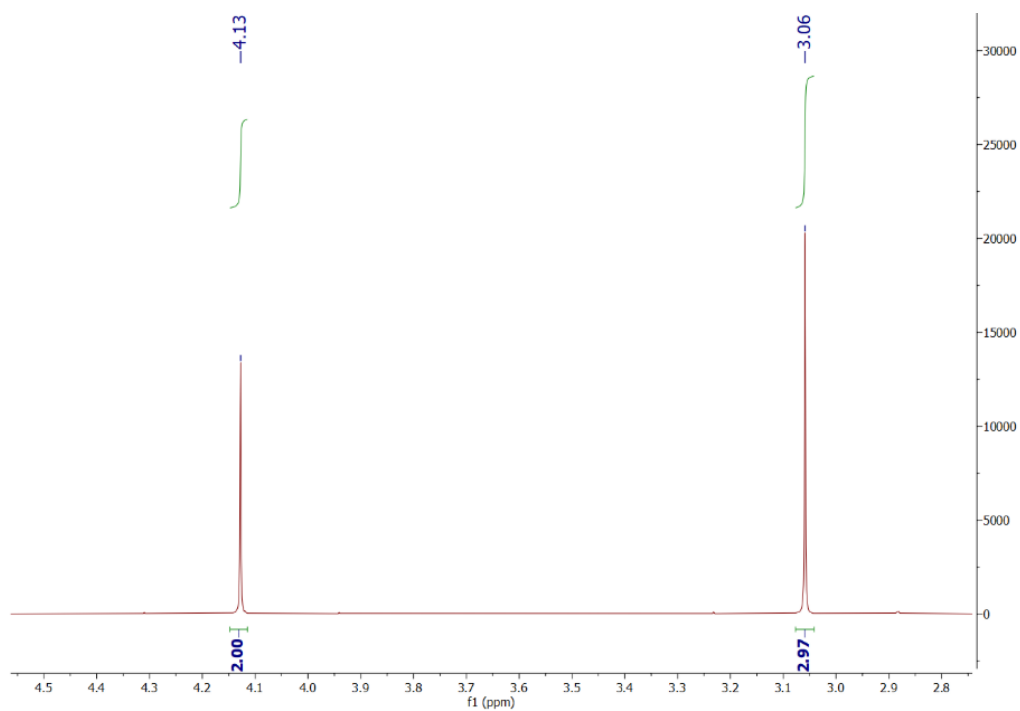


Figure S8:  $^1\text{H}$  NMR spectrum of Sar NCA.

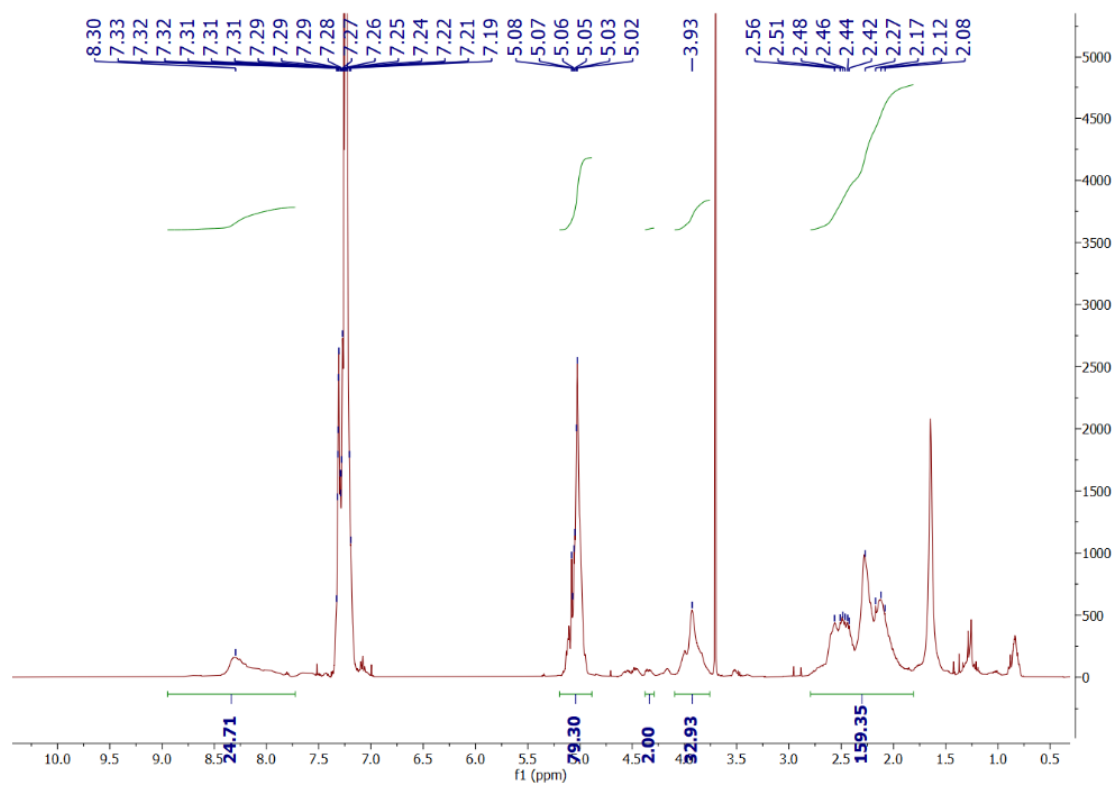


Figure S9:  $^1\text{H}$  NMR spectrum of PBLG<sub>40</sub>.

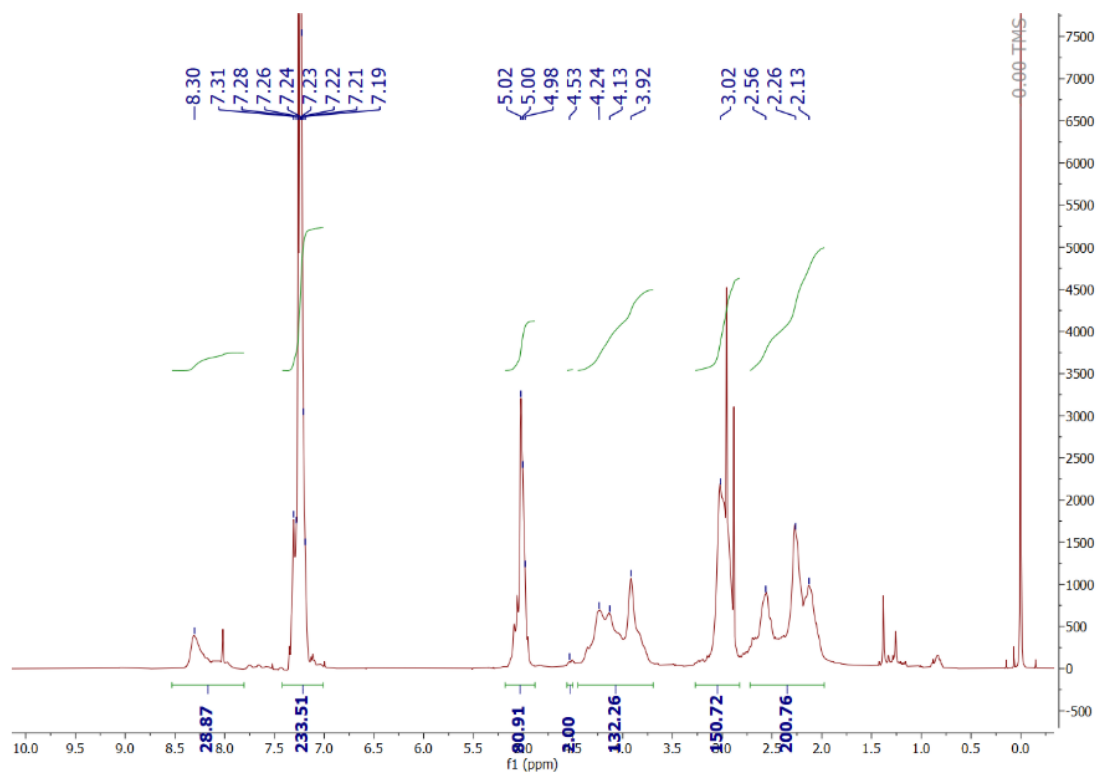


Figure S10:  $^1\text{H}$  NMR spectrum of PBLG<sub>40</sub>-b-PSar<sub>50</sub>.

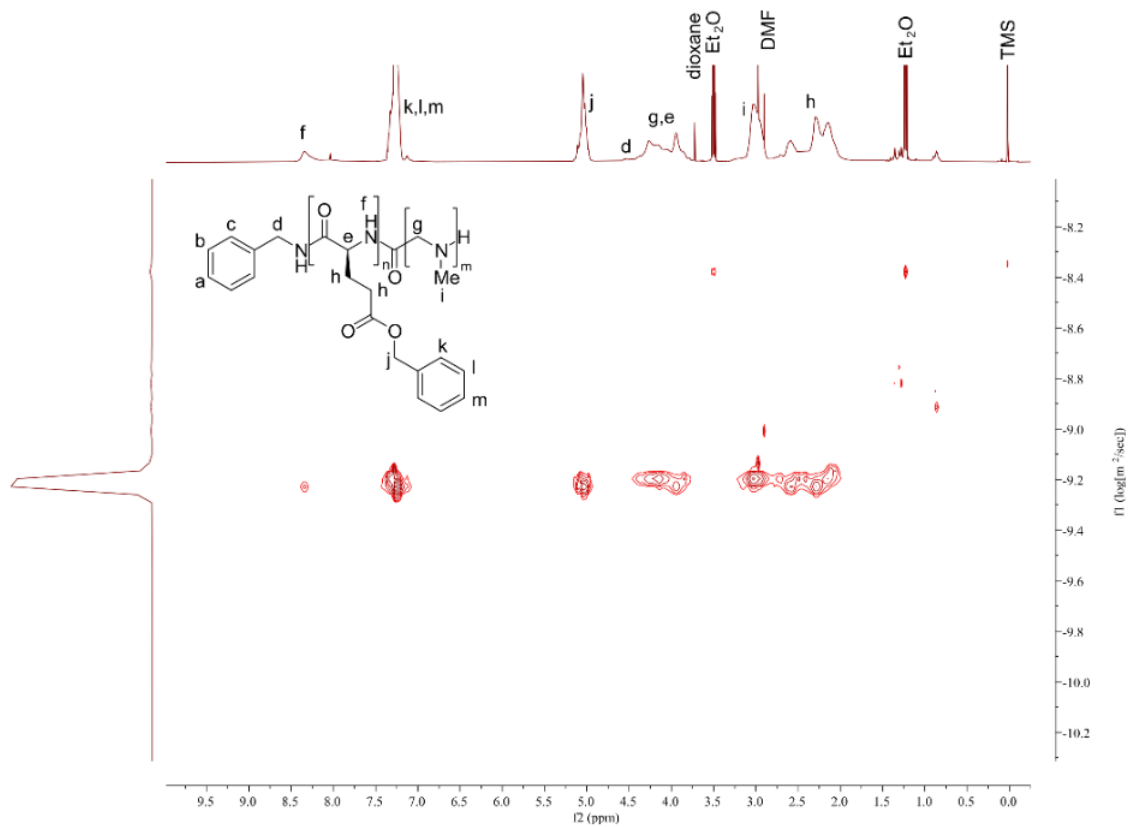


Figure S11: DOSY spectrum of PBLG<sub>40</sub>-b-PSar<sub>50</sub>.

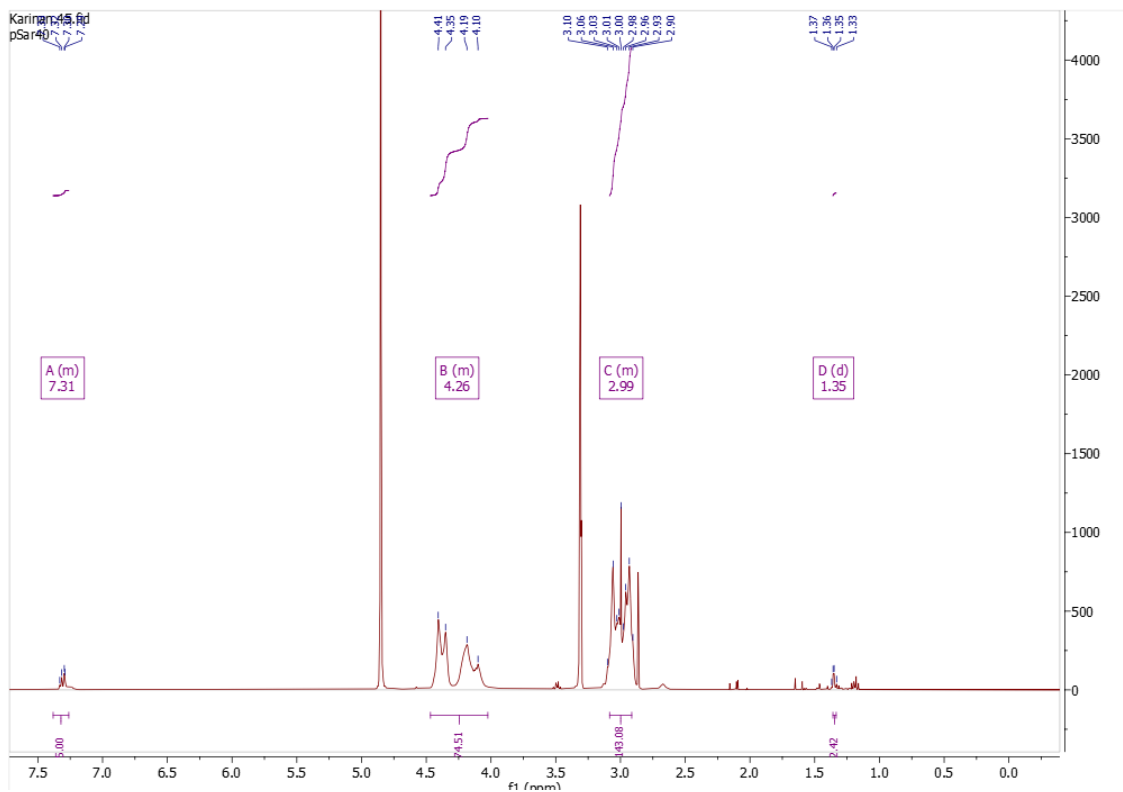
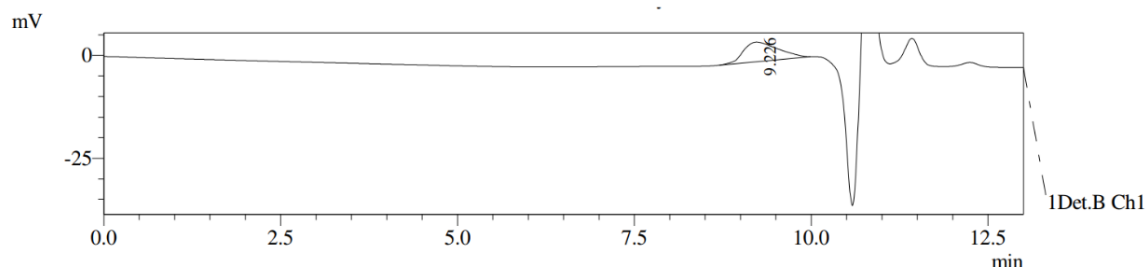


Figure S12: <sup>1</sup>H NMR spectrum of PSar<sub>40</sub>.

## Gel Permeation Chromatography

The polydispersity of the polymers was determined in THF.



**Figure S13:** GPC trace of PBLG<sub>40</sub>. The PDI was determined to be 1.04.

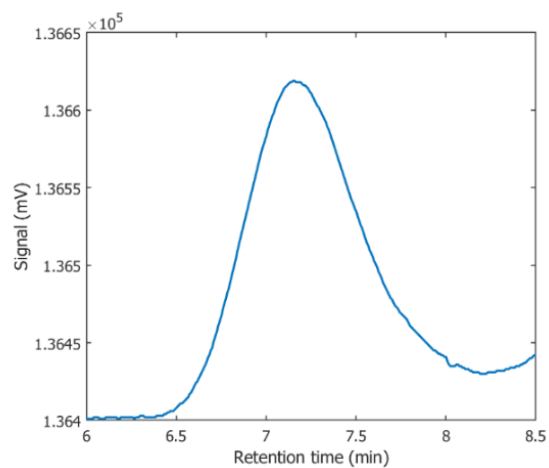


**Figure S14:** GPC trace of PBLG<sub>40</sub>-b-pSar<sub>50</sub>. The PDI was determined to be 1.07.

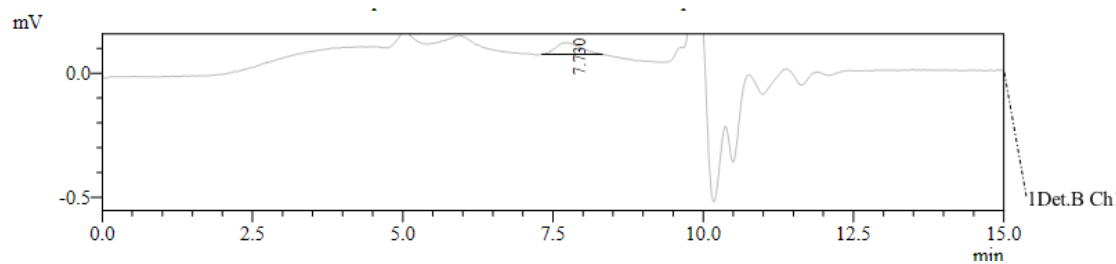


**Figure S15:** GPC trace PSar<sub>40</sub>. The PDI was determined to be 1.04.

## Differential Scanning Calorimetry

The thermogram for PSar<sub>50</sub>-PBLG<sub>40</sub> was measured at a rate of 10 °C/min. The first heating cycle was from 20 °C to 120 °C and then back to 20 °C. The second and third heating cycle were both from 20 °C to 180 °C and back to 20 °C. The resulting thermogram can be seen in (**Figure S16**) with an indication for the peak of the dehydration at 72 °C and glass transition at 105 °C.

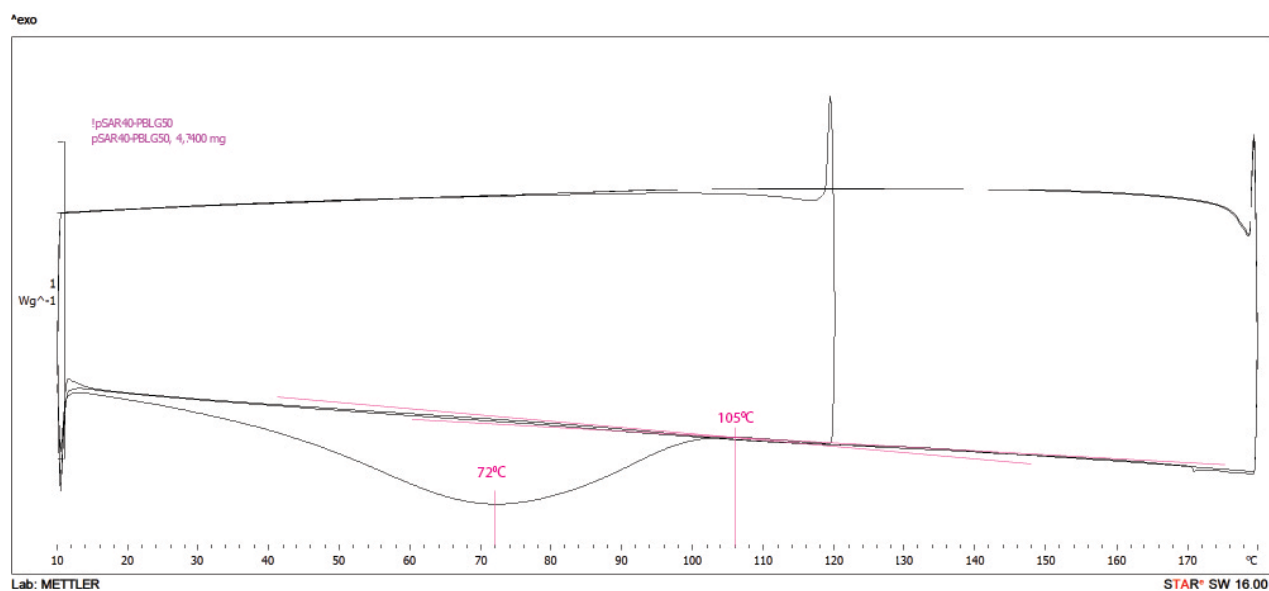


**Figure S16:** Thermogram of PBLG<sub>40</sub>-PSar<sub>50</sub> with the peak for dehydration at 72 °C and the glass transition temperature at 105 °C.

## TEM and Cryo-TEM images

### TEM sample preparation and analysis

The self-assembled suspension in MQ water (0.5 mg/ml), 5  $\mu$ L was pipetted onto the carbon coated TEM grid. The suspension was left to sit for 1 min before removing the liquid using a filter paper. Subsequently, 1% PTA staining (3  $\mu$ L) was pipetted onto the TEM grid and left to sit for 1 min before being removed by filter paper. The TEM grid was then left to dry for at least 4 h before analysis. The TEM samples were analysed on a JEOL TEM-1400Flash operated at 80 kV equipped with a Matataki Flash sCMOS camera.

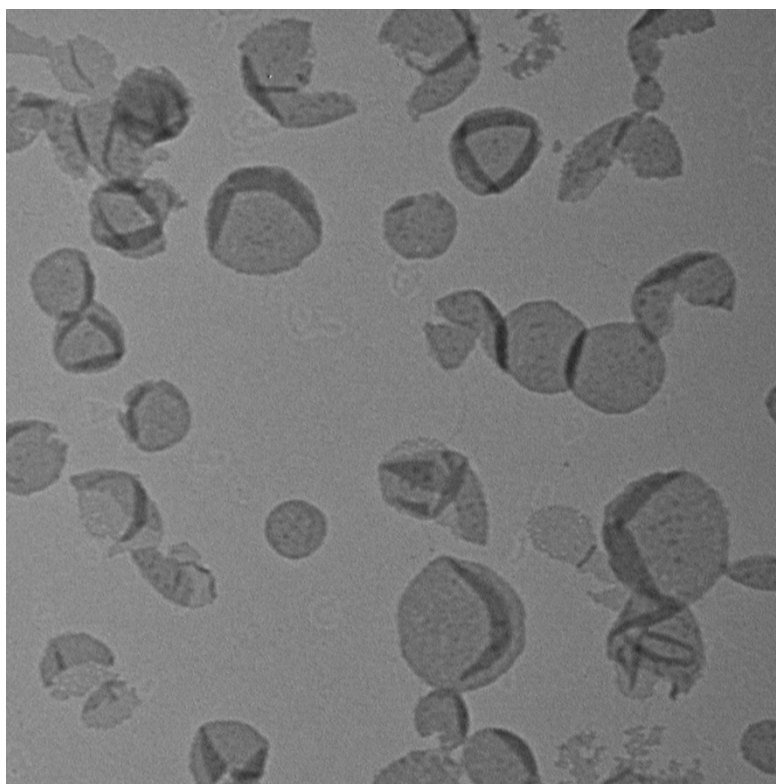


**Figure S17:** TEM image of PBLG<sub>40</sub>-b-PSar<sub>50</sub> polymersome. PTA staining was used.

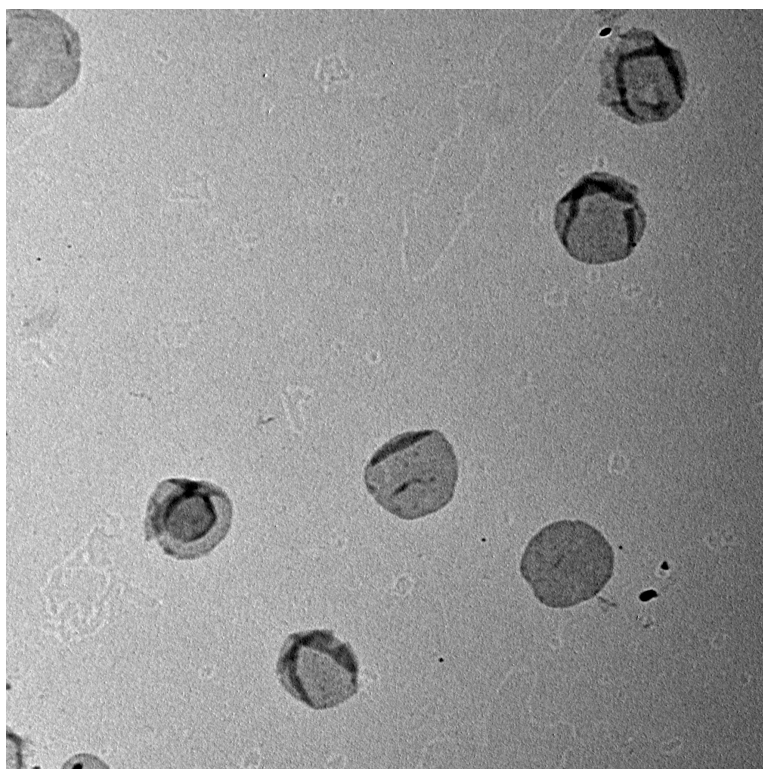


**Figure S18:** TEM image of shape transformation of PBLG<sub>40</sub>-b-PSar<sub>50</sub> at 70°C, quenched after 1 minute. PTA staining was used.

### TEM HFIP Self-assembly

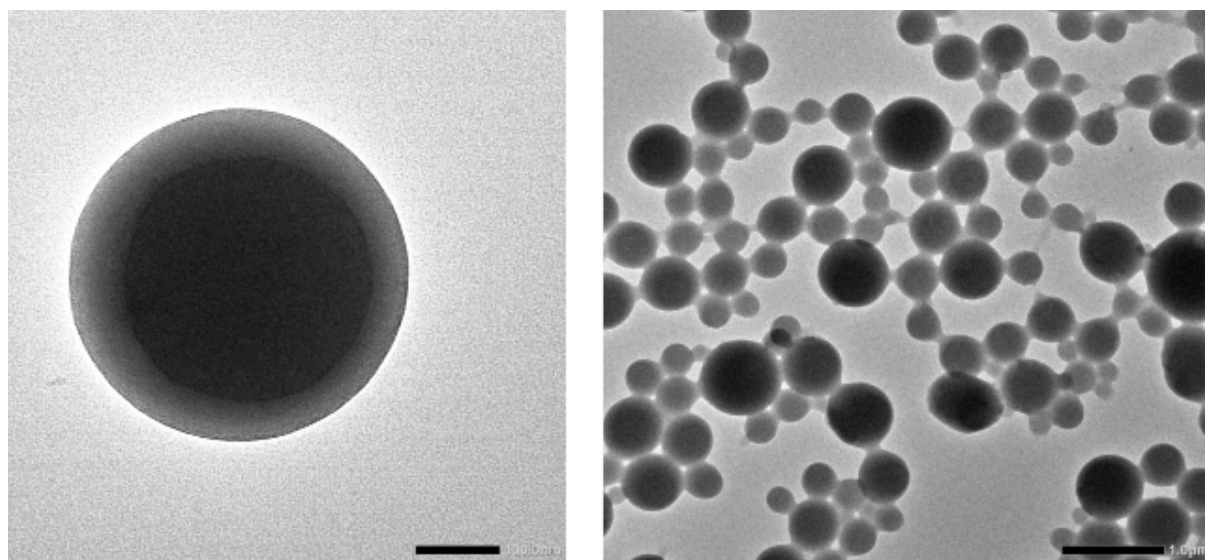


**Figure S19:** TEM images of vesicles assembled in HFIP; the vesicles have a much darker appearance compared to vesicles assembled in DMF.

## Cryo-TEM sample preparation and analysis

The carbon-coated holey film supported by a copper grid (R2/2 Cu200) was first treated with plasma at 15 kV for 40 seconds. The grid was then placed in a controlled climate chamber at 20 °C with a relative humidity near saturation. Five microliters of the vesicle sample (approximately 5 mg/ml) were deposited onto the grid, which was subsequently rapidly frozen in liquid ethane at -180 °C and then transferred to liquid nitrogen at -196 °C. The specimen was then transferred to a JEOL TEM 2100 using a cryo holder. The acceleration voltage was set to 200 kV.

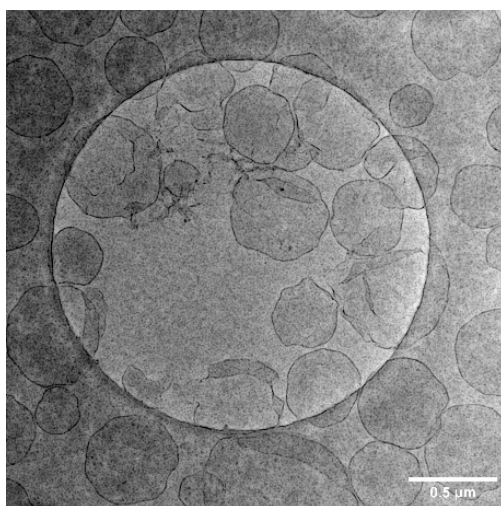


**Figure S20:** Cryo TEM image of PBLG<sub>40</sub>-b-PSar<sub>50</sub> vesicles.

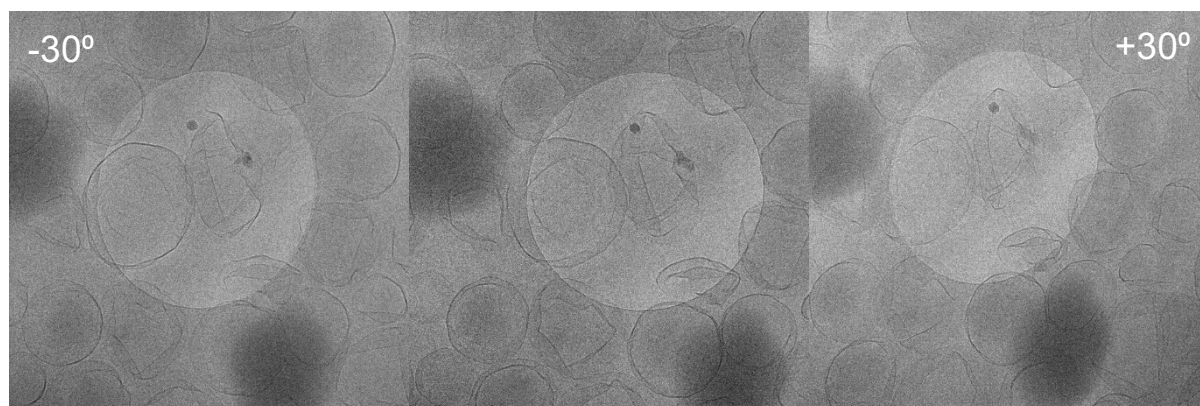


**Figure S21:** Cryo TEM image of PBLG<sub>40</sub>-b-PSar<sub>50</sub> vesicles after 1 min of PEG addition at room temperature, with the left and right panel being -30° and +30° respectively.

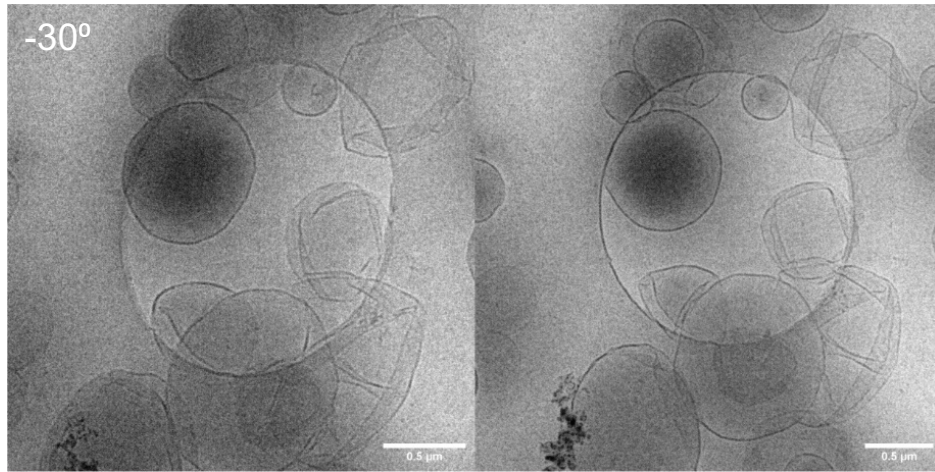


**Figure S22:** Cryo TEM image of PBLG<sub>40</sub>-b-PSar<sub>50</sub> vesicles after 1 min of PEG addition at 60°C, with the left panel being -30°.

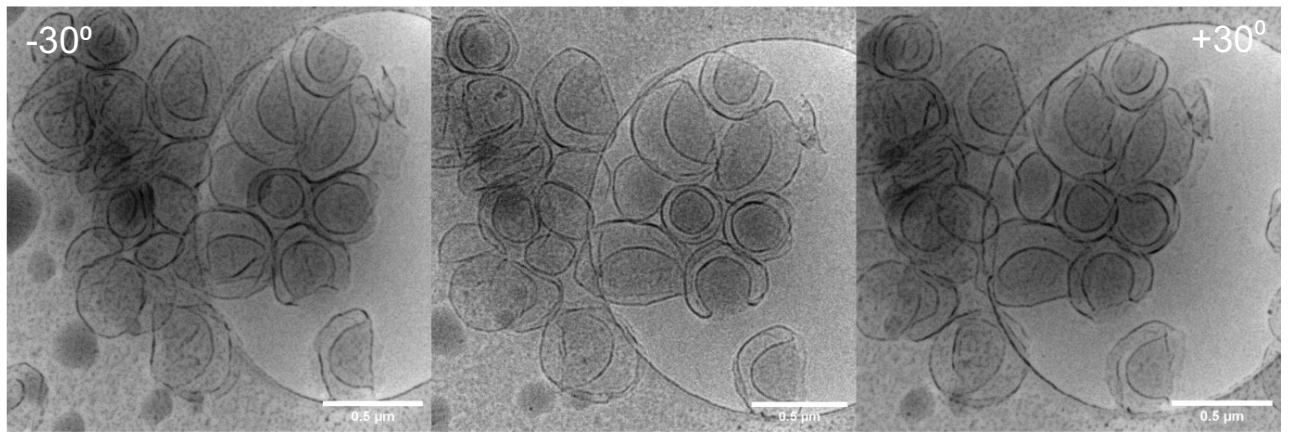


**Figure S23:** Cryo TEM image of PBLG<sub>40</sub>-b-PSar<sub>50</sub> vesicles after 1 min of PEG addition at 70°C, with the left and right panel being -30° and +30° respectively.

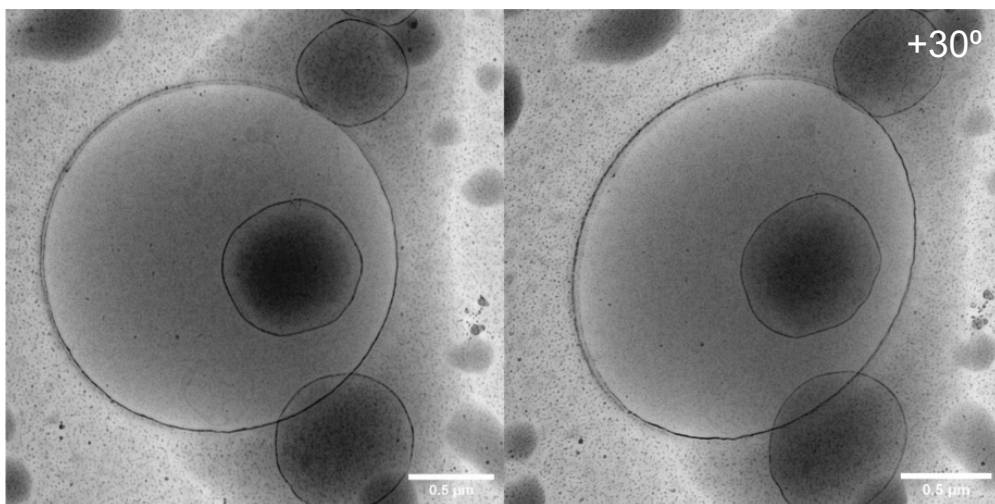


**Figure S24:** Cryo TEM image of PBLG<sub>40</sub>-b-PSar<sub>50</sub> vesicles after 1 min of PEG addition at 75°C, with the right panel +30°.

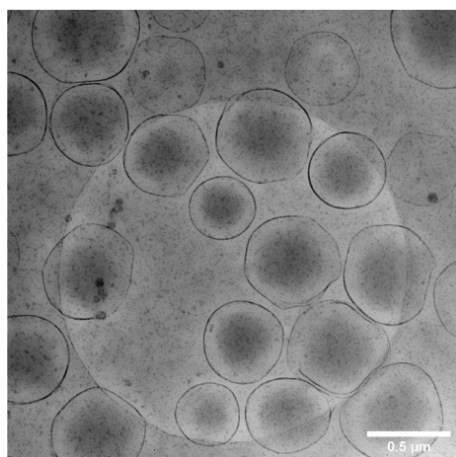


**Figure S25:** Cryo TEM image of PBLG<sub>40</sub>-b-PSar<sub>50</sub> vesicles after 1 min of PEG addition at 80°C.

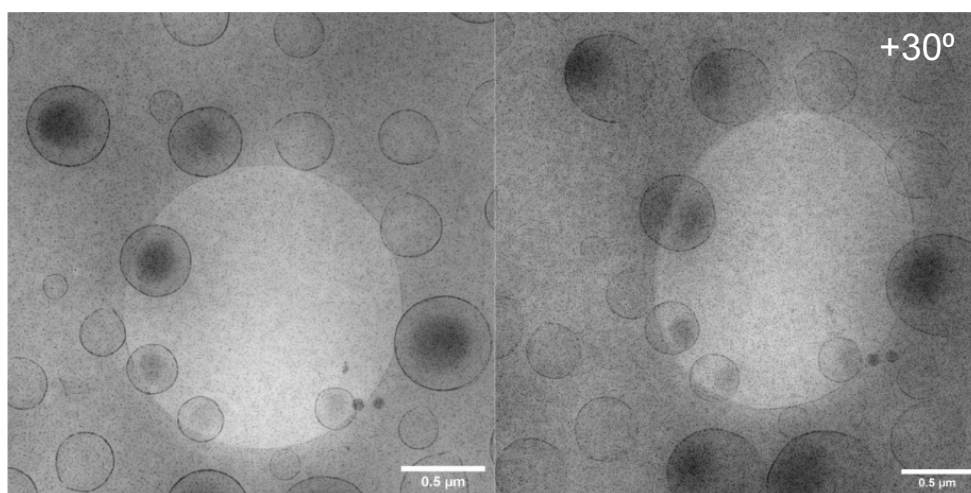


**Figure S26:** Cryo TEM image of PBLG<sub>40</sub>-b-PSar<sub>50</sub> vesicles after dialyses at 70°C with the right panel at +30°.

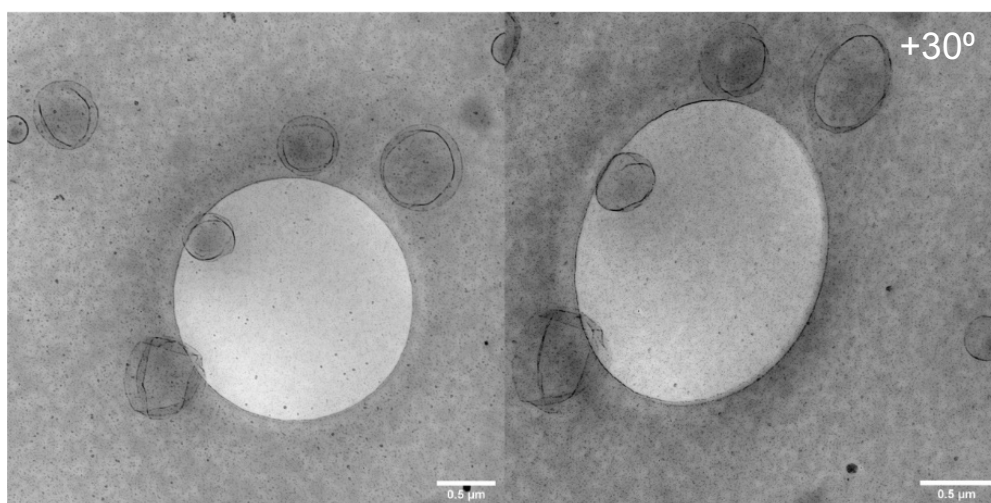


**Figure S27:** Cryo TEM image of PBLG<sub>40</sub>-b-PSar<sub>50</sub> vesicles after 2 min of PEG addition at 70°C, with the right panel at +30°.

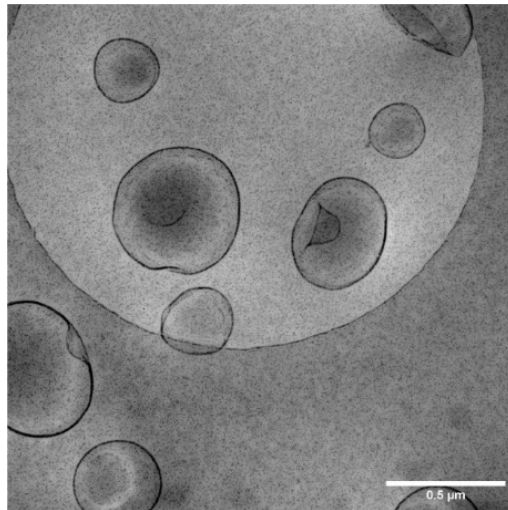


**Figure S28:** Cryo TEM image of PBLG<sub>40</sub>-b-PSar<sub>50</sub> vesicles after 5 sec of PEG addition at 70°C.

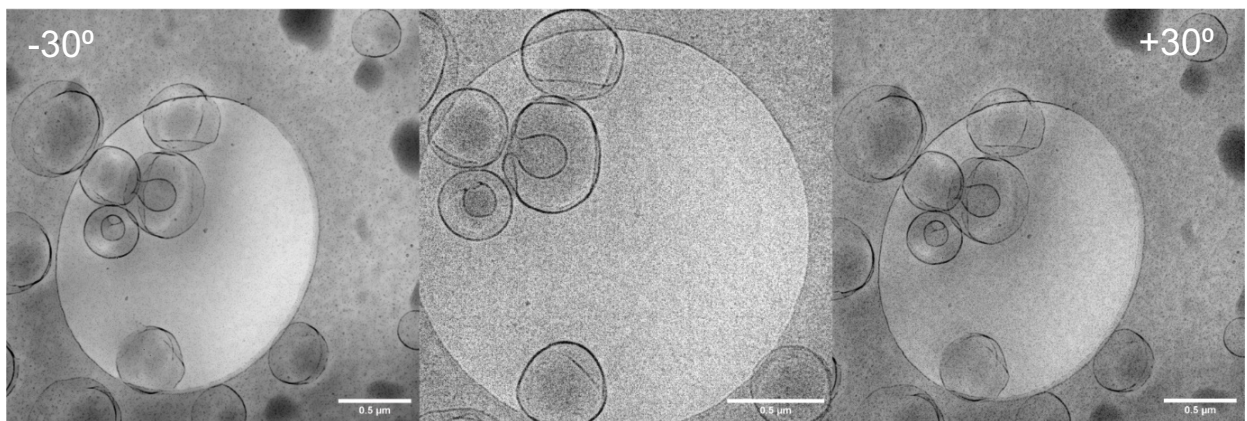


**Figure S29:** Cryo TEM image of PBLG<sub>40</sub>-b-PSar<sub>50</sub> vesicles after 30 sec of PEG addition at 70°C, with the left and right panel being -30° and +30° respectively.

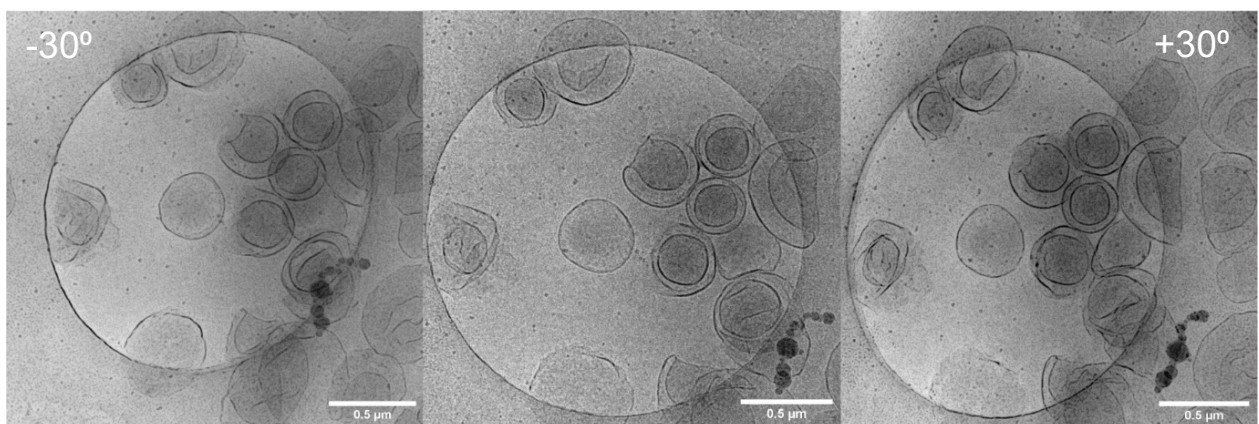


**Figure S30:** Cryo TEM image of PBLG<sub>40</sub>-b-PSar<sub>50</sub> vesicles after 1 min of PSar addition at 70°C, with the left and right panel being -30° and +30° respectively.

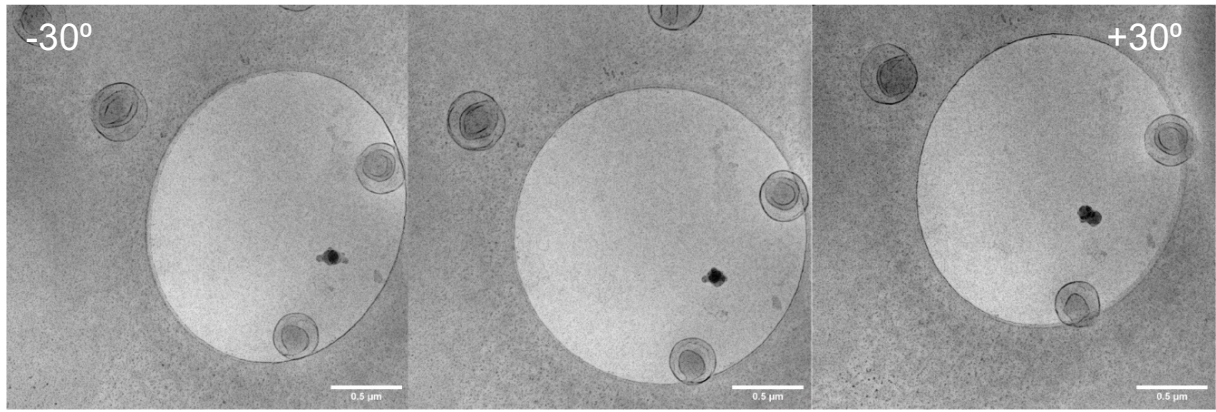


**Figure S31:** Cryo TEM image of PBLG<sub>40</sub>-b-PSar<sub>50</sub> vesicles after 1 min of saccharose addition at 70°C with the left and right panel being -30° and +30° respectively.

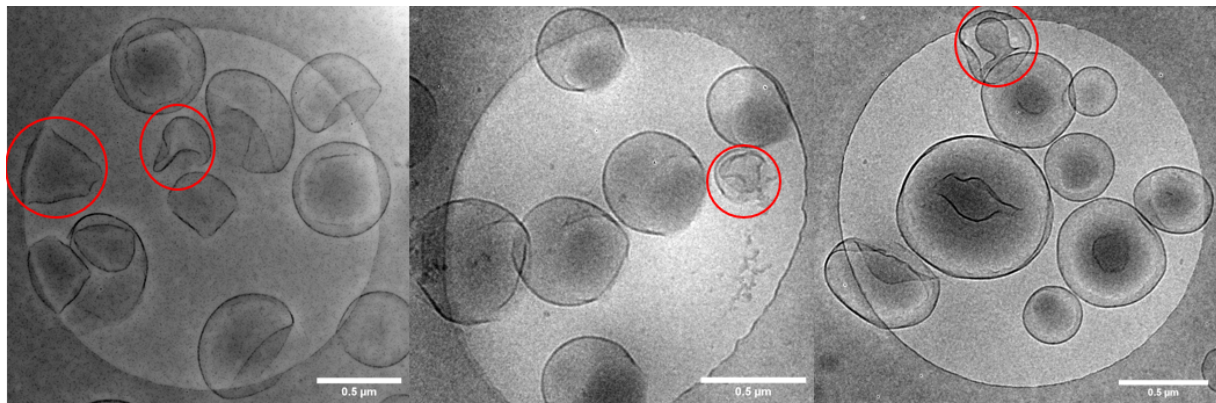


**Figure S32:** Some structures found between 5 and 30 seconds of PEG addition can have an anomalous shape. These shapes can also be found as metastable shapes of red blood cells[2].

# Behaviour of the membrane study

## Temperature interval of PBLG<sub>40</sub>-b-pSar<sub>50</sub> polymersome on DLS

The polymersomes were dissolved in MilliQ and the size was measured continuously at different temperatures in *triplo* general purpose data processing. The data points are spaced out with 10 °C interval.

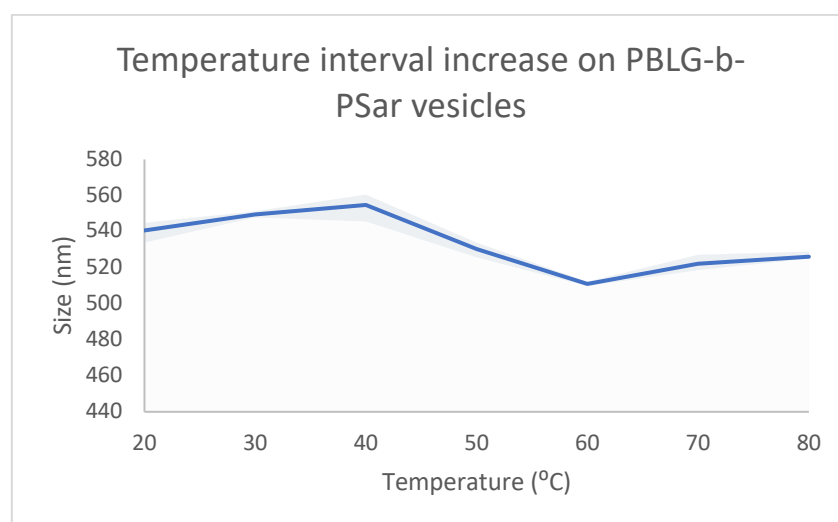


**Figure S33:** DLS temperature interval experiment on PBLG<sub>40</sub>-b-PSar<sub>50</sub> vesicles with increasing temperature from 20°C to 80°C shows the average size of the vesicles. Experiments were done in *triplo*.

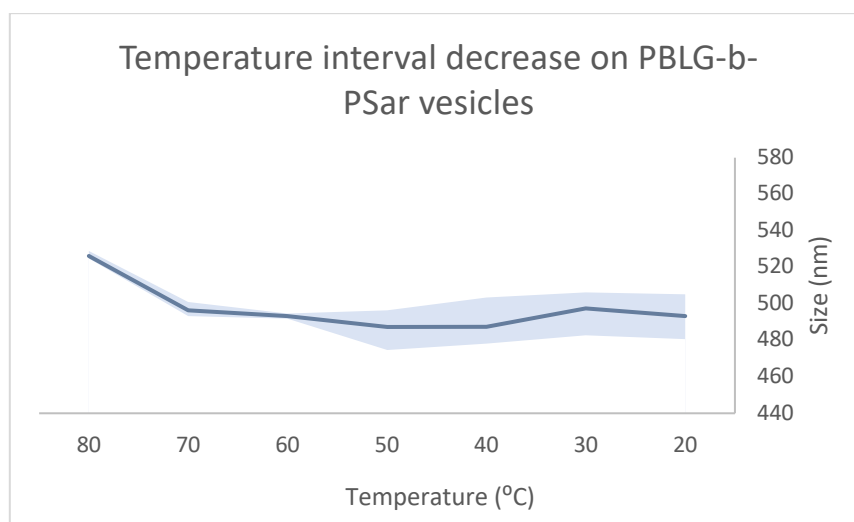


**Figure S34:** DLS temperature interval experiment on PBLG<sub>40</sub>-b-PSar<sub>50</sub> vesicles with decreasing temperature from 80°C to 20°C shows the average size of the vesicles. Experiments were done in *triplo*.

**Table S3:** Temperature interval experiment on DLS with polymersome of PBLG<sub>40</sub>-b-PSar<sub>50</sub> data points

| Temperature (°C) | Average size (nm) |
|------------------|-------------------|
| 20               | 540.7             |
| 30               | 549.5             |
| 40               | 554.7             |
| 50               | 530.3             |
| 60               | 510.9             |
| 70               | 522.0             |
| 80               | 521.5             |
| 70               | 496.4             |
| 60               | 493.2             |
| 50               | 487.4             |
| 40               | 479.3             |
| 30               | 497.4             |
| 20               | 493.2             |

## Temperature interval of PBLG<sub>40</sub>-b-pSar<sub>50</sub> polymersome on CD

Parameters for the measurement of these vesicles include an accumulation of five measurements with a scanning speed of 200 nm/min and a D.I.T. of 0.5 seconds. For the temperature interval, a 5.0 °C data pitch was used with a 2 °C temperature gradient with a delay time of 20 seconds.

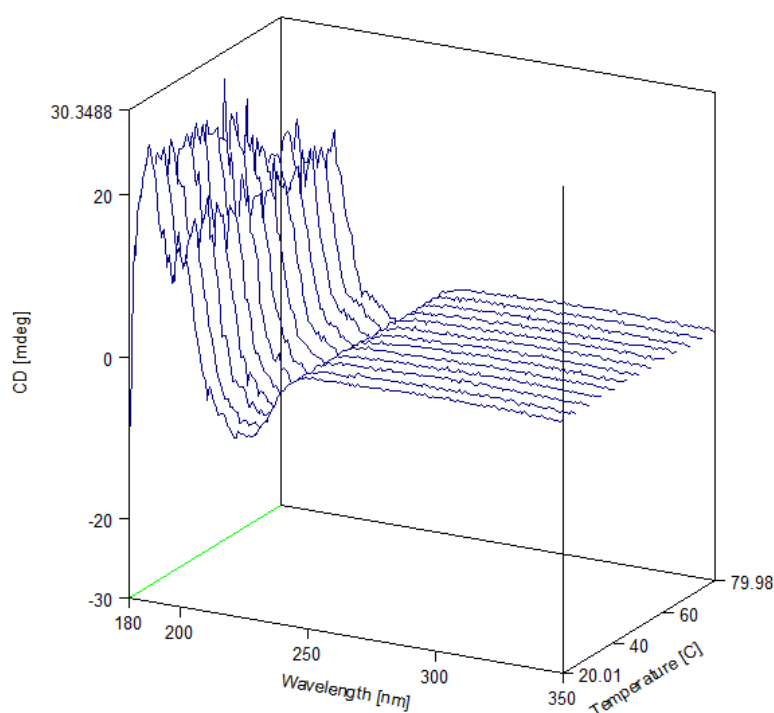


**Figure S35:** Temperature interval measurement of PLBG<sub>40</sub>-b-PSar<sub>50</sub> on CD

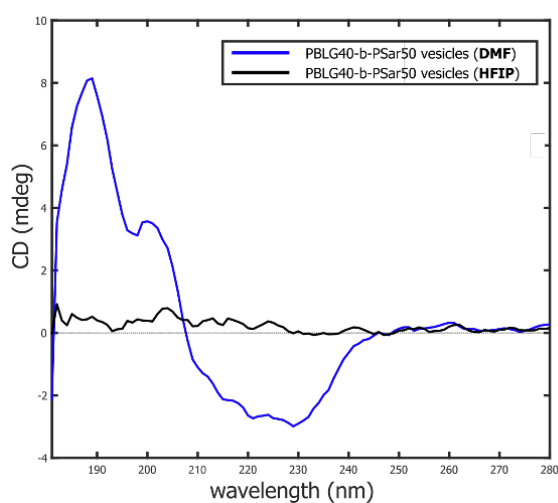


**Figure S36:** Vesicles assembled in DMF and HFIP have a different CD spectrum, the difference could be caused by a different packing of the polymer in the membrane.

## Pyrene fluorescence temperature dependence

10 mM PSar-PBLG vesicles were dissolved in MilliQ with the addition of 0.05 mM pyrene. The sample was excited at 355nm. The parameters include an accumulation of three measurements with a scanning speed of 200 nm/min and a D.I.T. of 0.5 seconds. For the temperature interval, a 5.0 °C data pitch was used with a 2 °C temperature gradient with a delay time of 20 seconds. In Figure S37 the fluorescent spectra of pyrene in presence of the PSar-PBLG vesicles at 20°C and 80°C. There are two peaks visible but the most clear difference can be seen at 361.4nm and 361.8nm. The ratio between those peaks at the different temperatures can be used to determine when the hydrophobicity of the membrane changes as seen in Figure 3b.

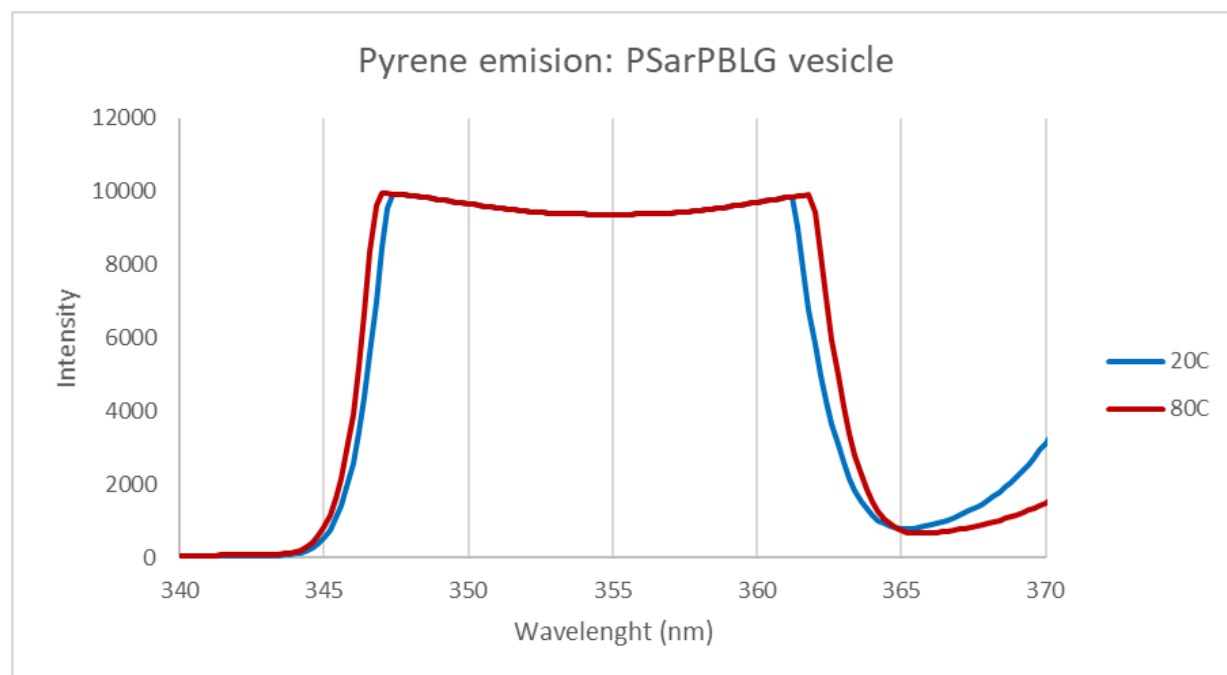


**Figure S37:** The fluorescent spectra of pyrene in the presence of PSar-PBLG vesicles at 20°C and 80°C having peaks at 361.4 nm and 362.8 nm respectively.

## Critical Micelle Concentration

The critical micelle concentration was determined for PBLG<sub>40</sub>-b-PSar<sub>50</sub> with the help of NanoSight. A dilution series was prepared from a solution of 4 mg of polymer in 1 ml of MilliQ. Starting from the lowest concentration the particle count was measured and plotted in (Figure S38). The intersection of the lines was calculated to be between the concentrations 0.044 and 0.10 mg/ml.

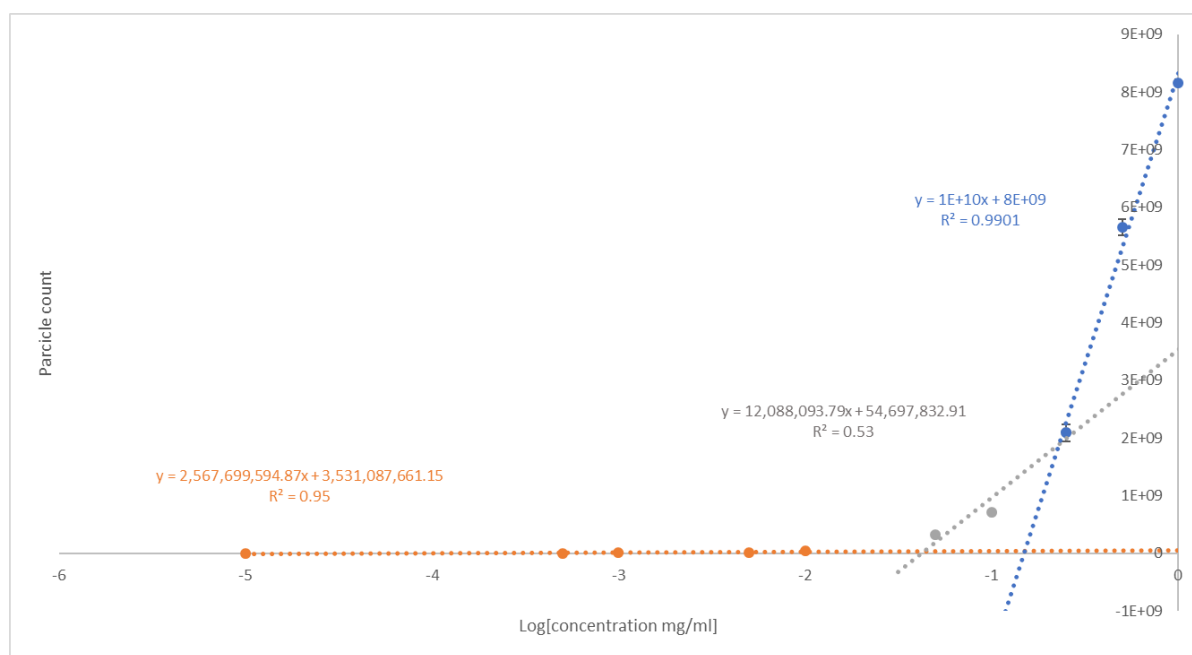


**Figure S38:** The plotted of critical micel concentration for PBLG<sub>40</sub>-b-PSar<sub>50</sub>, with on the y axis particle count and on the x axis the log of the polymer concentration.

## Stability and degradation study

To function as drug delivery vehicles, vesicles should be both biocompatible and biodegradable[3, 4]. The speed at which the degradation occurs is of high importance for drug delivery vehicles. If the vesicles are degraded too quickly, the cargo will be released too soon and will not reach the target of interest in the body[4]. Additionally, for biomedical applications it is desirable that vesicles have a decent shelf-life and can be stored either at room temperature (RT), in the fridge or in the freezer for future use[5]. Therefore, we set out to study the stability of PBLG<sub>40</sub>-b-PSar<sub>50</sub> vesicles under different conditions.

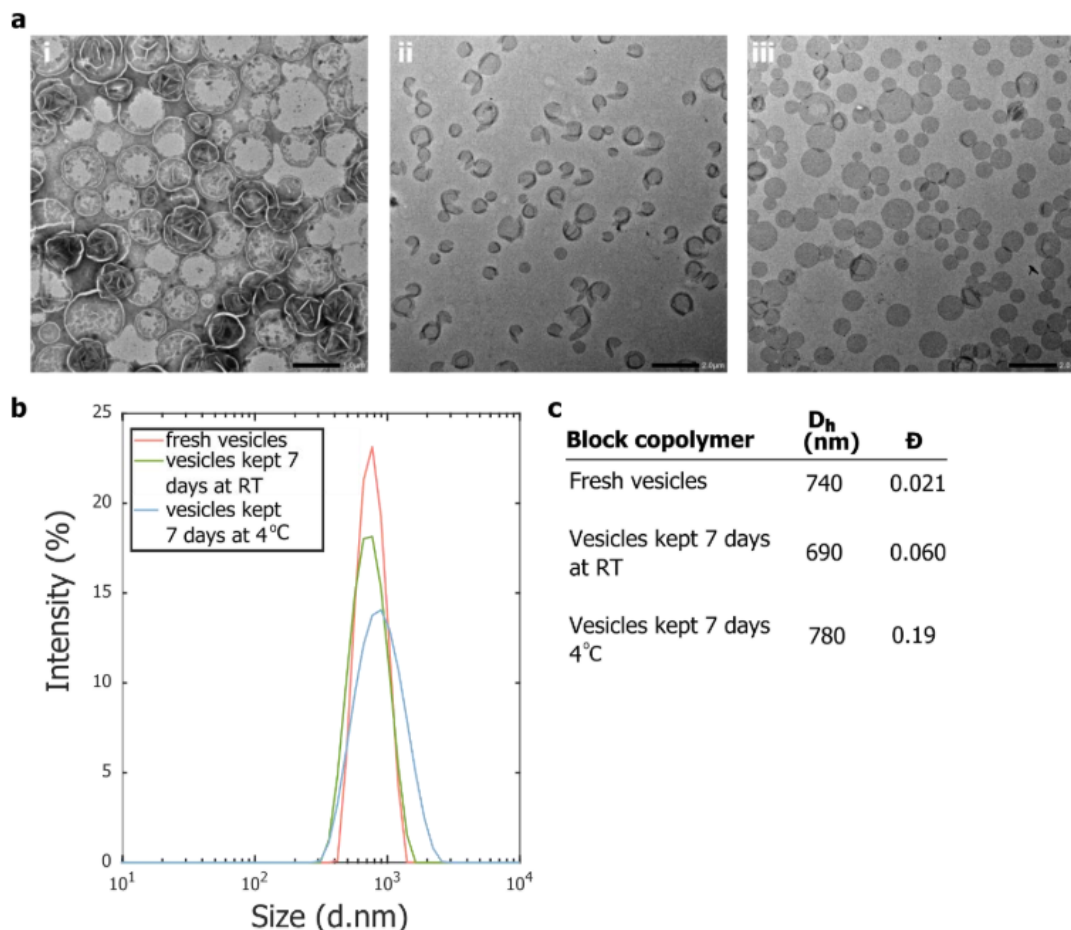


**Figure S39:** Stability of PBLG<sub>40</sub>-b-PSar<sub>50</sub> vesicles in MQ water. a) TEM images of i) freshly prepared vesicles, ii) vesicles stored at room temperature for 7 days, and iii) vesicles stored at 4 °C for 7 days. For all TEM samples PTA was used as negative stain. b) Size distributions by DLS of vesicles kept under different conditions. c) Table of characteristics of vesicles kept at different temperatures determined by DLS.

## Stability of PBLG<sub>40</sub>-b-PSar<sub>50</sub> vesicles

To study the stability of PBLG<sub>40</sub>-b-PSar<sub>50</sub> vesicles and examine its shelf-life, one batch of vesicles was prepared in DMF and stored at different temperatures for up to 7 days in MQ water. When kept at RT for 7 days, it was observed that the vesicles displayed a different morphology than the freshly prepared vesicles (**Figure S39-i,ii**). After 7 days at RT the vesicles seem more ruptured and disintegrated compared to the freshly prepared vesicles (**Figure S39a-i,ii**). Furthermore, it was also observed that the vesicles shrink in size compared to the freshly prepared vesicles by ~50 nm (**Figure S1Figure S39a-ii, c**). Additionally, it was determined that the dispersity of the vesicles had also increased compared to the freshly prepared vesicles (**Figure S39c**). Interestingly, for the vesicles that were stored at 4 °C for 7 days, a limited change in morphology was observed compared to the freshly prepared vesicles (**Figure S39**). However, an increase in size of ~40 nm was observed, and an increase in dispersity compared to the freshly prepared vesicles (**Figure S39**). We believe that the difference in morphology between the freshly prepared vesicles and the vesicles stored at 4 °C on one hand, and the vesicles stored at RT on the other hand, is due to the difference in solubility of the polymer at different temperatures in water [6].

At RT, the solubility of the polymer in water is expected to be larger than at 4 °C. The increased solubility of the polymer at RT could lead to a decreased stability of the vesicle leading disintegration of the vesicle. Moreover, it was expected that the increase in size that was observed for vesicles stored at 4 °C compared to the fresh vesicles, is due to water uptake of the vesicles over time. The reason this phenomenon is not observed for vesicles stored at RT, could be the result of the disintegration of the vesicles, which would increase the permeability, but at the same time phase out the membrane pressure. This would lead to no size increase of the vesicles.

The apparent decrease in size of the vesicles stored at RT could be due to DLS measurement errors, as DLS works suboptimal for non-spherical particles [7]. As can be seen from the cryoTEM images of the PBLG<sub>40</sub>-b-PSar<sub>50</sub> vesicles, these vesicles are not perfectly spherical even when freshly prepared (**Figure S17**). The permeability of the vesicles at different temperatures must be quantified in order to confirm this notion. This could be achieved by incorporation of a dye (e.g. NileRed) into the vesicles and quantifying the diffusion of the dye for vesicles at different temperatures through (confocal) microscopy.

### Three-week stability study

Inspired by the one-week stability study, a new batch of vesicles and also a batch of stomatocytes were prepared and stored at 4 different temperatures. These particles were monitored with DLS and TEM for 21 days. The vesicles were stored in the fridge at a temperature of 4 °C, at room temperature (~20 °C), at 37 °C and lastly at 70 °C.

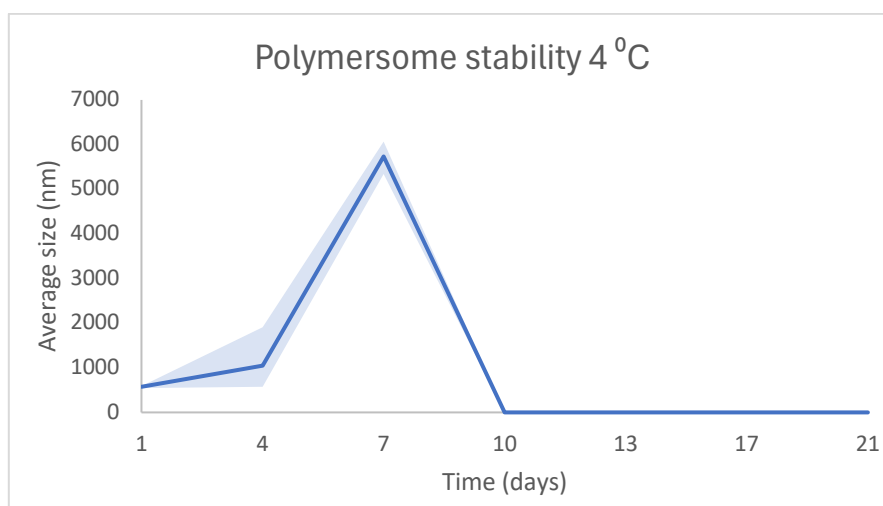


**Figure S40:** DLS stability study of PBLG<sub>40</sub>-b-PSar<sub>50</sub> polymersomes over 21 days at 4 °C. After 10 days, no more polymersomes are observed.

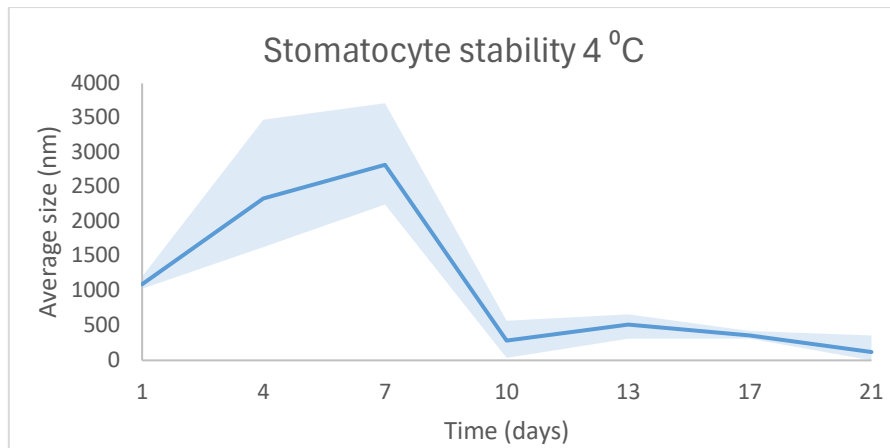


**Figure S41:** DLS stability study of PBLG<sub>40</sub>-b-PSar<sub>50</sub> stomatocytes over 21 days at 4 °C. The stomatocytes show a large size distribution and the average size goes down drastically after 7 days.

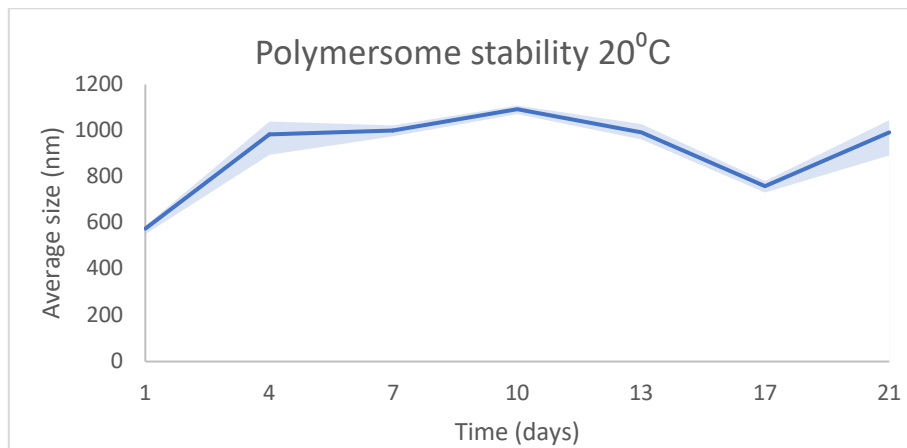


**Figure S42:** DLS stability study of PBLG<sub>40</sub>-b-PSar<sub>50</sub> polymersomes over 21 days at 20 °C. The polymersomes appear to show good stability over the full duration of the experiment.

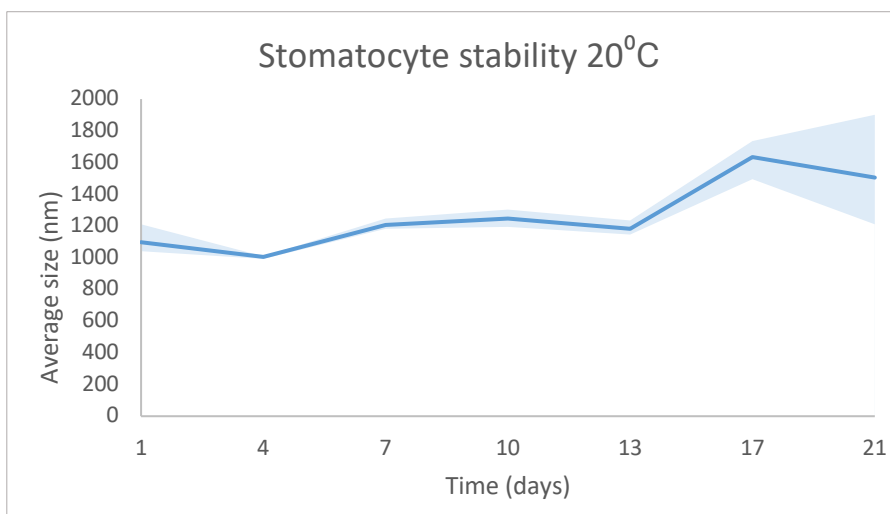


**Figure S43:** DLS stability study of PBLG<sub>40</sub>-b-PSar<sub>50</sub> stomatocytes over 21 days at 20 °C. The stomatocytes appear to show good stability up to 17 days, after this there is an increase in size distribution.

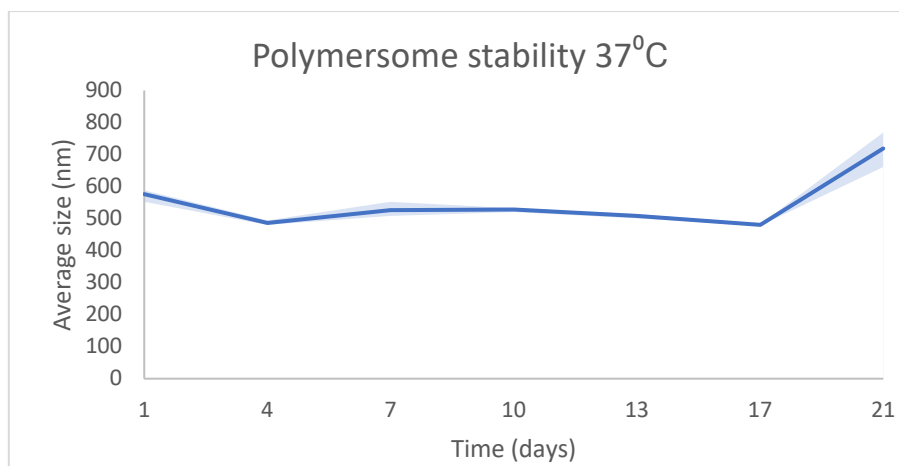


**Figure S44:** DLS stability study of PBLG<sub>40</sub>-b-PSar<sub>50</sub> polymersomes over 21 days at 37 °C. The polymersomes appear to show good stability up to 17 days.

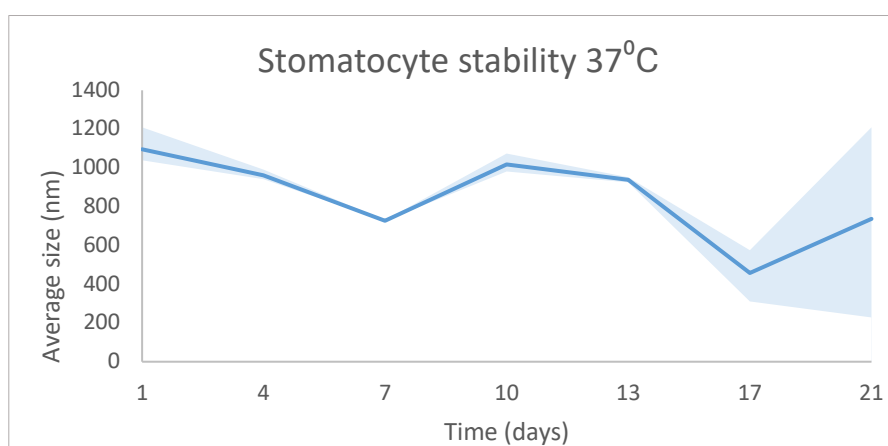


**Figure S45:** DLS stability study of PBLG<sub>40</sub>-b-PSar<sub>50</sub> stomatocytes over 21 days at 37 °C. The stomatocytes appear to show good stability at the start. However, at 17 days the size distribution greatly increases.

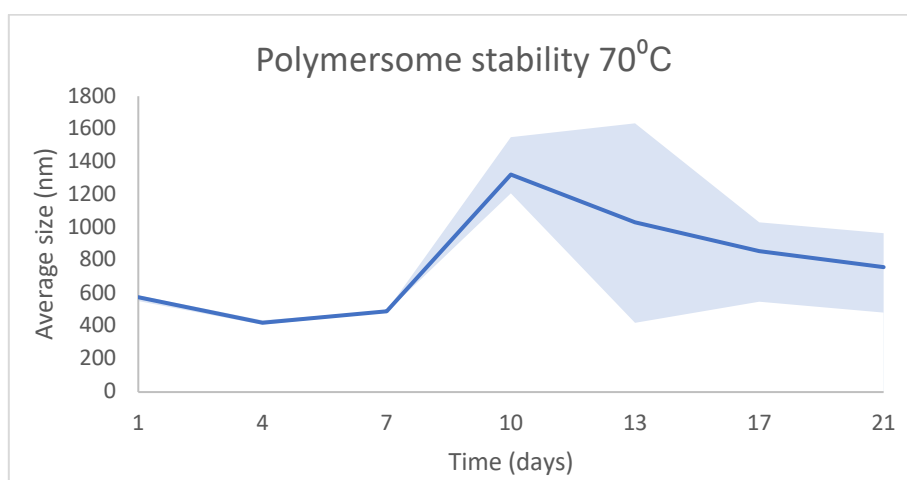


**Figure S46:** DLS stability study of PBLG<sub>40</sub>-b-PSar<sub>50</sub> polymersomes over 21 days at 70 °C. A significant increase in size distribution can be observed from day 13 onwards.

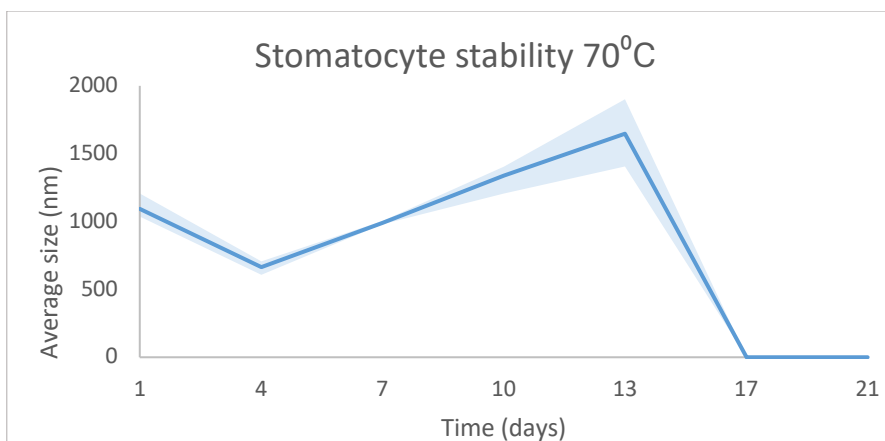


**Figure S47:** DLS stability study of PBLG<sub>40</sub>-b-PSar<sub>50</sub> stomatocytes over 21 days at 70 °C. The stomatocytes appear to show good stability at the start. However, at 17 days no more stomatocytes were observed.

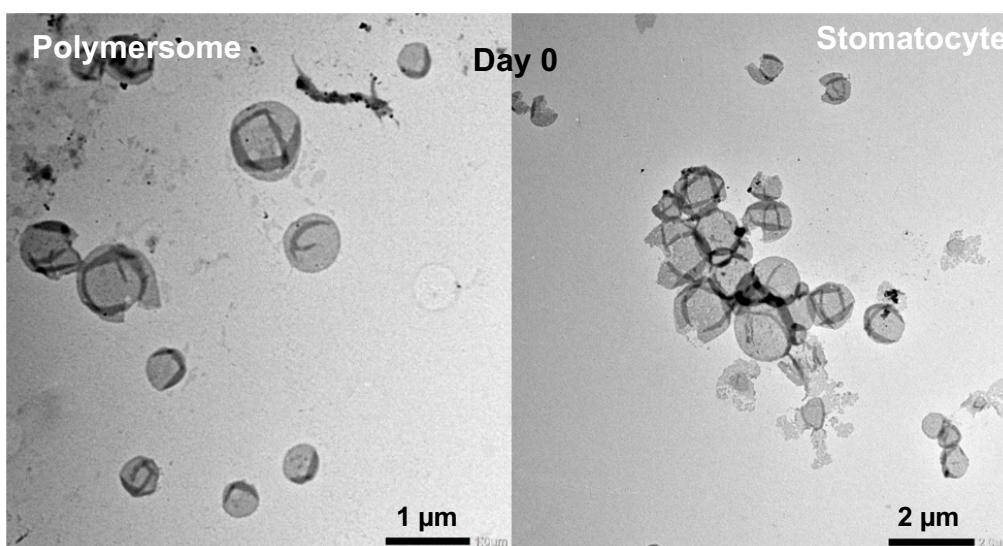


**Figure S48:** TEM images of polymersomes (left) and stomatocyte (right) at the start of the stability study. PTA staining was used.

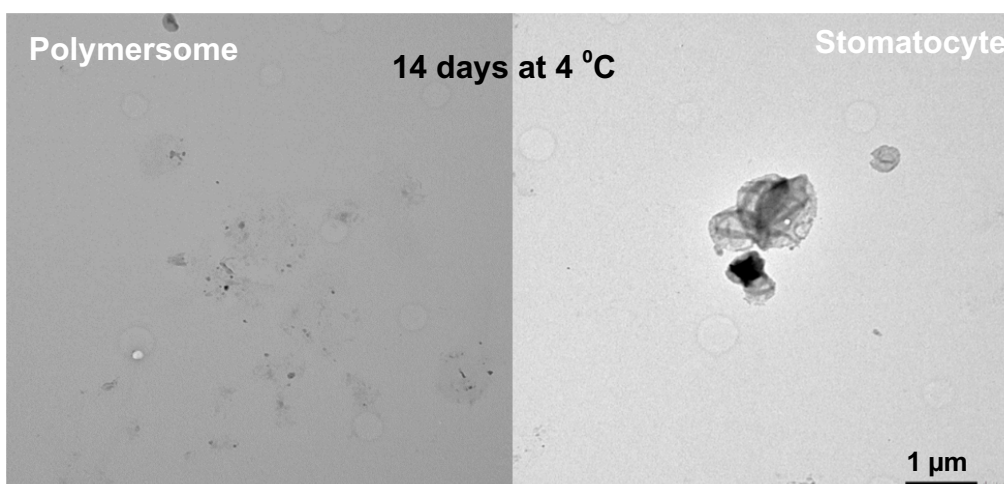


**Figure S49:** TEM images of polymersomes (left) and stomatocytes (right) that were stored at 4 °C. Images were taken after 14 days. Very few vesicles could be seen. PTA staining was used.

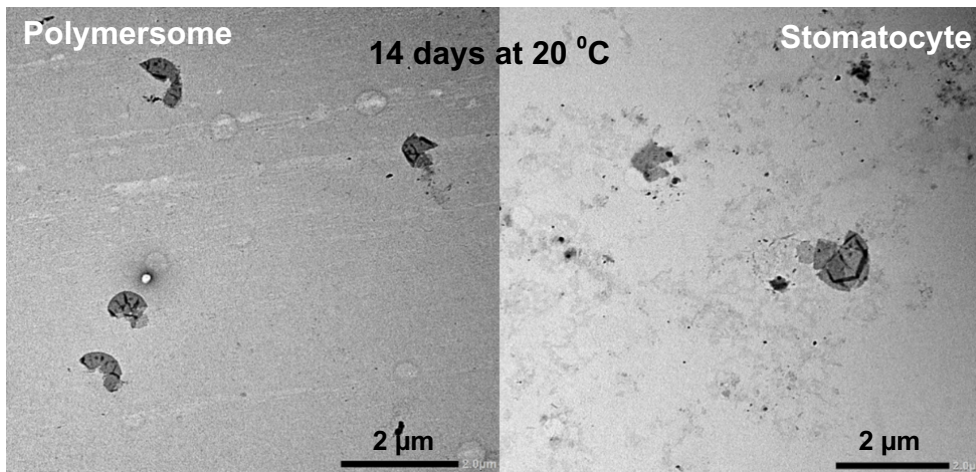


**Figure S50:** TEM images of polymersomes (left) and stomatocytes (right) that were stored at 20 °C. Images were taken after 14 days. Many vesicles were observed. PTA staining was used.

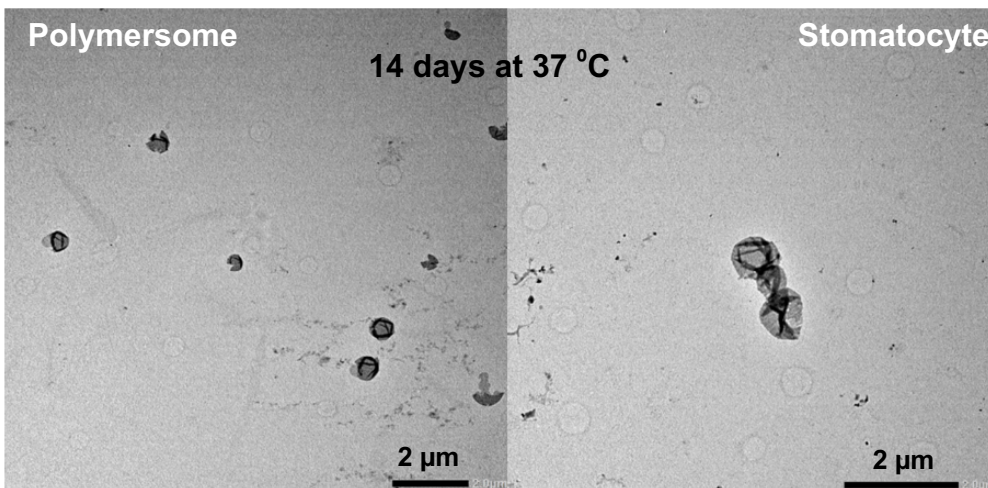


**Figure S51:** TEM images of polymersomes (left) and stomatocytes (right) that were stored at 37 °C. Images were taken after 14 days. Many vesicles were observed. PTA staining was used.

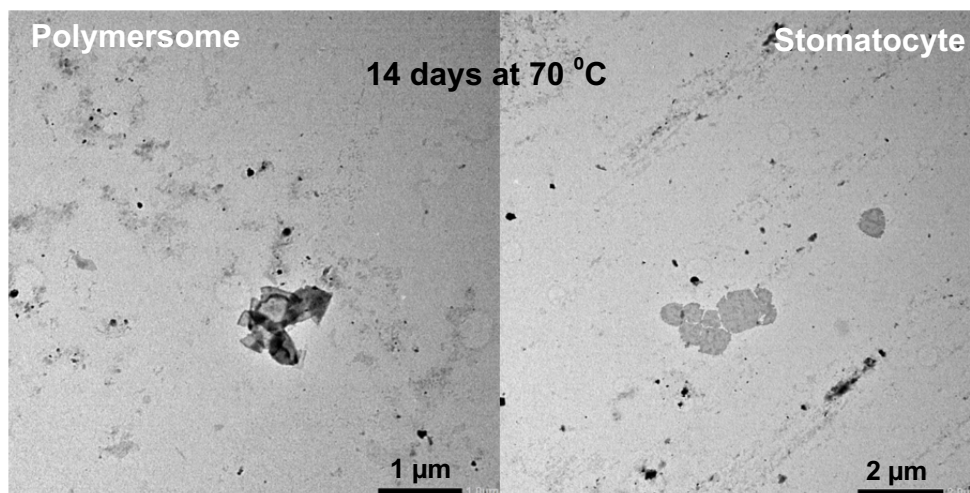


**Figure S52:** TEM images of polymersomes (left) and stomatocytes (right) that were stored at 37 °C. Images were taken after 14 days. Few vesicles were observed. PTA staining was used.

From the DLS and TEM results it can be seen that PBLG<sub>40</sub>-b-PSar<sub>50</sub> vesicles can be stored at any temperature up to 7 days, with minimal disintegration and no morphological changes. For longer storage, room temperature and 37 °C seem to give the most stability to the vesicles in terms of size and concentration of intact vesicles. It could be observed from TEM imaging that the number of vesicles that could be found during the imaging went down with longer storage.

Overall, we expect that PBLG<sub>40</sub>-b-PSar<sub>50</sub> vesicles provide a promising stepping stone to towards the facile fabrication of degradable vesicles for biomedical applications with a decent shelf-life.

### **Degradability of PBLG<sub>40</sub>-b-PSar<sub>50</sub> vesicles**

Over the last few years, amphiphilic polypeptides have received considerable attention for use as a new class of nanocarriers for drug delivery[8] due to their exceptional degradability [9] and biocompatibility [10].

Polypeptides have been extensively shown to have low immunogenicity, low cytotoxicity, and biodegradability leading to their attraction for biomaterials research.[11] It has been shown in literature that PBLG containing polypeptides show biodegradable properties when incubated in PBS (pH 7.4) in the presence and absence of trypsin at 37 °C [12, 13] and in the enzymatic presence of Pseudomonas lipase. [14]

A similar class to polypeptides is polypeptoids. While polypeptides have a chiral side chain on their backbone  $\alpha$ -carbon, polypeptoids have an achiral side chain on their amide nitrogen. This leads to a lower protease susceptibility and subsequent lower biodegradability. These properties are favourable for applications that require sustained resistance times, such as drug delivery.

Because of the achirality of poly(sarcosine), the polypeptoid is more resistant to protease, more stable and degrades slower. The substitution on the amide nitrogen also limits hydrogen bonding between the polymers, which enhances the solubility of the polymer in water and alters the chain conformation. The achirality aids in the exhibition of disordered structures, in contrast to peptidic  $\alpha$ -helices and  $\beta$ -sheets.

Poly(sarcosine) is a non-ionic and highly hydrophilic poly (amino acid) or polypeptoids has shown many advantages when compared to PEG, e.g. high water solubility, easy synthesis and functionality, and neglect immunogenicity. [15-18] PSar is considered to be the only existing polymer synthesized from endogenous substances, rendering it extremely safe for human use. Meanwhile, PSar is able to be degraded under acid or enzymatic environment [15].

## References

1. Rasouli, M., *Basic concepts and practical equations on osmolality: Biochemical approach*. Clinical biochemistry, 2016. **49**(12): p. 936-941.
2. Lim, H.W.G., M. Wortis, and R. Mukhopadhyay, *Stomatocyte-discocyte-echinocyte sequence of the human red blood cell: evidence for the bilayer-couple hypothesis from membrane mechanics*. Proc Natl Acad Sci U S A, 2002. **99**(26): p. 16766-9.
3. Herrmann, I.K., M.J.A. Wood, and G. Fuhrmann, *Extracellular vesicles as a next-generation drug delivery platform*. Nature nanotechnology, 2021. **16**(7): p. 748-759.
4. Wilson, D.A., R.J. Nolte, and J.C. Van Hest, *Autonomous movement of platinum-loaded stomatocytes*. Nature chemistry, 2012. **4**(4): p. 268-274.
5. Peng, F., Y. Tu, and D.A. Wilson, *Micro/nanomotors towards in vivo application: cell, tissue and biofluid*. Chemical Society Reviews, 2017. **46**(17): p. 5289-5310.
6. Castro, F.L.A.d., et al., *Temperature and curing time affect composite sorption and solubility*. Journal of Applied Oral Science, 2013. **21**: p. 157-162.
7. Levin, A.D., E.A. Shmytkova, and B.N. Khlebtsov, *Multipolarization dynamic light scattering of nonspherical nanoparticles in solution*. The Journal of Physical Chemistry C, 2017. **121**(5): p. 3070-3077.
8. Stevens, C.A., K. Kaur, and H.-A. Klok, *Self-assembly of protein-polymer conjugates for drug delivery*. Advanced Drug Delivery Reviews, 2021. **174**: p. 447-460.
9. Liu, Z., et al., *Self-assembled biodegradable protein-polymer vesicle as a tumor-targeted nanocarrier*. ACS applied materials & interfaces, 2014. **6**(4): p. 2393-2400.
10. Vandermeulen, G.W. and H.A. Klok, *Peptide/protein hybrid materials: enhanced control of structure and improved performance through conjugation of biological and synthetic polymers*. Macromolecular Bioscience, 2004. **4**(4): p. 383-398.
11. Hutchinson, F. and B. Furr, *Biodegradable polymer systems for the sustained release of polypeptides*. Journal of Controlled Release, 1990. **13**(2-3): p. 279-294.
12. Tian, H., et al., *Biodegradable cationic PEG-PEI-PBLG hyperbranched block copolymer: synthesis and micelle characterization*. Biomaterials, 2005. **26**(20): p. 4209-4217.
13. Li, L., et al., *In situ polymerization of poly ( $\gamma$ -benzyl-L-glutamate) on mesoporous hydroxyapatite with high graft amounts for the direct fabrication of biodegradable cell microcarriers and their osteogenic induction*. Journal of Materials Chemistry B, 2018. **6**(20): p. 3315-3330.
14. Le Hellaye, M., et al., *Biodegradable polycarbonate-b-polypeptide and polyester-b-polypeptide block copolymers: synthesis and nanoparticle formation towards biomaterials*. Biomacromolecules, 2008. **9**(7): p. 1924-1933.
15. Birke, A., J. Ling, and M. Barz, *Polysarcosine-containing copolymers: Synthesis, characterization, self-assembly, and applications*. Progress in Polymer Science, 2018. **81**: p. 163-208.

16. Alberg, I., et al., *Polymeric nanoparticles with neglectable protein corona*. *Small*, 2020. **16**(18): p. 1907574.
17. Makino, A., et al., *Control of in vivo blood clearance time of polymeric micelle by stereochemistry of amphiphilic polydepsipeptides*. *Journal of controlled release*, 2012. **161**(3): p. 821-825.
18. Weber, B., et al., *PeptoSomes for Vaccination: Combining Antigen and Adjuvant in Polypeptide-Based Polymersomes*. *Macromolecular Bioscience*, 2017. **17**(10): p. 1700061.